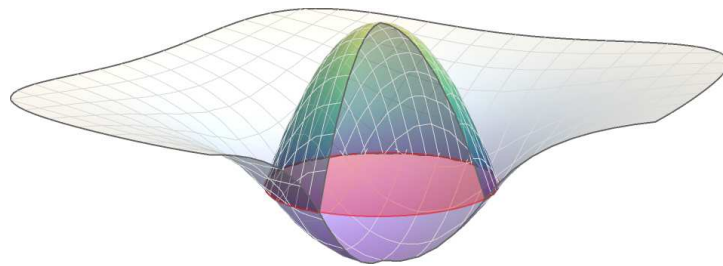# Ultraviolet regular Black Holes

Master Thesis

Sven Köppel

October 2014

Supervisor: PD Dr. Piero Nicolini
Second supervisor: Prof. Dr. Marcus Bleicher

Institute for theoretical Physics &
Frankfurt Institute for Advanced Studies

GOETHE
UNIVERSITÄT
FRANKFURT AM MAIN

Vorliegende Version ist vom **October 10, 2014, 18:05**

Abstract

In this thesis, I present a family of Black Hole geometries exposing a modified minimal length scale behaviour due to the gravity self-complete paradigm. I extend these geometries to the ADD large extra-dimensional scenario. This allows black hole remnant masses to reach the TeV scale. We show that the evaporation endpoint for this class of Black holes is a cold stable remnant. While the one geometry features a regular deSitter core that counters gravitational collapse with a quantum outward pressure, the other geometry turns out to fit nicely into the holographic information bound on black holes, leading to black hole area quantization and applications in the black hole entropic force, deriving gravity as emergence phenomenon from the fundamental thermodynamics.

The thesis contains an overview about recent quantum gravity black hole approaches and concludes with the derivation of nonlocal operators that modify the Einstein equations to ultra-violet safe field equations.

Master thesis

written at

Institut für theoretische Physik
Fachbereich Physik
Goethe-Universität Frankfurt am Main
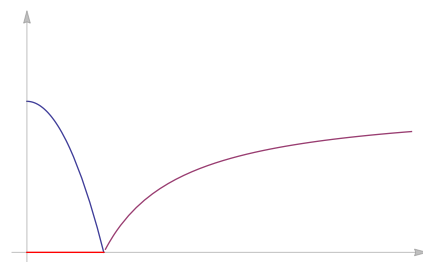Max-von-Laue-Straße 1
60438 Frankfurt am Main

and

Frankfurt Institute for Advanced Studies (FIAS)
Ruth-Moufang-Straße 1
60438 Frankfurt am Main

About the front picture

The 3-dimensional illustration shows an embedding of the equitorial plane of a self-regular black hole, which gravitational potential is e.g. shown in figure 4.4 for $\alpha \to \infty$. For the sake of better understanding, there is a cut-out to view the inside of the object. Mathematically, the picture shows a two dimensional surface embedded in three dimensions, but actually every point represents a 2-sphere (in 4d spacetime). It can be constructed by rotating the graph shown on the right around it's y axis.

Contents

1 Introducion

This work is about the quest of contemporary physics on the smallest scales and with the biggest energies. By historical evolution, in the 20th century two opposing theories developed: Quantum physics, which is the physics at smallest scales and produced confusing paradoxa like Schrödinger's cat, and on the other hand relativistic physics, which is physics at the biggest scales and lead to general relativity, the theory for space and time presented by Albert Einstein in 1915.

The combination of Quantum mechanics and special relativity lead to Quantum Field Theory (QFT) and the formulation of the standard model of particle physics which is exceptionally and unexpectedly successful. From the viewpoint of an high-energy physicist, three of four fundamental interactions, namely the electromagnetic, weak nuclear and strong nuclear interactions have been successfully joined in a unified theory, and gravity is simply the weakest and last interaction left as an "ordinary" field theory. On the other hand, from the viewpoint of a relativist, general relativity tought us that there is no background space where physics "happens". This new principle lead to a bunch of new physics, where the most remarkable is perhaps the existence of black holes as trapped areas in spacetime or even the existence of wormholes (the Einstein-Rosen bridge). Certainly, General Relativity had the bigger impact on the science fiction genre.

Physics beyond the Standard model is an uncomfortable job. On the one hand, such physics lack experimental accessibility. Theoretically, the best thing we can do starting from QFT is curved space quantum field theory, that is, calculating quantum fields on a curved space background, but without space-matter interaction. In the *cube of physical theories*, as shown in figure 1.1, this is probably the half way to the "Theory of Everything".

Actually, curved space QFT opened the door for the first quantum mechanical treatments of strong gravitational objects: black holes. In the 1970s, this lead to Hawking's groundbreaking prediction of thermal radiation of Schwarzschild black holes. In terms of "theories", Hawking radiation is really interdisciplinary:

$$T_{\mathrm{H}} = \frac{\hbar\, c^3}{8\pi\, G\, M k_{\mathrm{B}}}$$

There are quantum ingredients (Planck constant $\hbar$), special relativity ingredients (speed of light c), gravitational ingredients (Newton's constant G) and thermodynamics (Boltzmann constant k_B).

Figure 1.1: The *cube of physics*, a popular illustration about characteristic constants that describe the regime for physical phenomena. Taken e.g. from Penrose [57] or [Hossenfelder].

But Hawking's temperature also contains the failure of General Relativity: The temperature increases with decreasing mass M, since it is written in the denominator. Since radiating black holes loose mass, they get hotter and hotter. If there are black holes (and physicans are pretty sure there are), the universe should be hot, but it is not.

In this thesis, I propose modifications to general relativity dealing with this kind of *big mass* problem of general relativity. As in physics, big mass correspond with high energy and low distance, we use the term *Ultra-Violet*, coming from the wavy nature of light, to describe an high energy regime. This thesis deals with ultra-violet corrections of the most simple black holes possible, the Schwarzschild black hole.
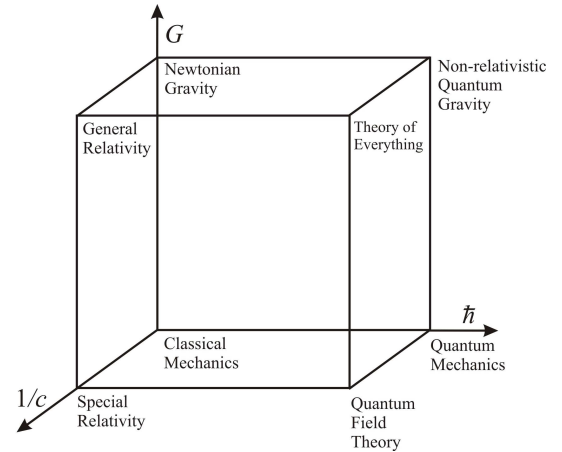
1.1   Structure of the thesis

Despite this introductory section, there will be another introduction section about General Relativity, section 2. This section collects text book knowledge and can be skipped by the advanced reader: We will give a short overview about the formalism and quickly derive the Einstein equation. Then we proceed to the first solutions on GR and discuss it's properties – it's the well-known Schwarzschild black hole, the starting point for all modifications in this thesis. I will also give an overview about topics in gravity in extra dimensions and finally discuss shortly the simplest class of empty spacetimes: Minkowski, DeSitter and Anti-DeSitter metrics.

Section 3 about static spherically symmetric solutions of GR is the first section with own results. We solve the Einstein Equations for an ideal static isotropic fluid and choose a blurred matter ball described by a radial mass profile as the starting point for black hole discussions. We call two special profiles the *holographic* and the *self-regular* mass profile.

In section 4, the geometry of such mass profiles is derived and discussed. We see the existence of Reissner-Nördstrom like ergospheres and the appearance of a stable Black hole *remnant*. We learn about the meaning of *self-encoding*, *self-completeness* and minimal length scales in gravity and study the regular DeSitter core of a black hole with its quantum interpretation.

In section 5, we continue to the thermodynamical properties of this class of black holes. We derive the associated temperature, heat capacity and entropy for such black holes and find a phase transition at some critical radius. Concerning the entropy, we learn about the meaning of *holography* in gravity and possible outcomes for the black hole information paradox.

In section 6, we finally modify Einstein equations with a nonlocal operator, finding a dual nonlocal gravity theory that gives the same results as the purely-Einsteinian matter. Such a theory may be called a *quantum improved* general relativity, as it incorporates short scale improvements in the context of tensor calculus and Riemannian geometry.

Chapter 2

Gravitation

2.1 General Relativity

In this section, I want to give a short introducion to General Relativity, which is the major theory used in this work. In the introductory part, we briefly retrace some core concepts of differential geometry on manifolds in favour to derive the Einstein equations. Afterwards, we discuss the properties of the Schwarzschild solution, which is the foundation for section 3.

The following sections serve the goal of retracing the lines of reasoning. A detailed and introductory, well defining discussion would go beyond the scope of this work. For readers unfamiliar with General Relativity, I recommend the introductory book by Thomas Fließbach [25], while I follow here the notation of the well-known text book by Robert Wald [71], who uses a more fundamental approach to introduce Riemannian geometry. Koch PhD [39]. Siehe auch Wald teaching [72].

2.1.1 Differential Geometry

In curved space geometry, intuition about well-known mathematical symbols like vectors as "position vectors" fails [72]. The mathematical approach is a differential description using the fact that manifolds M look "nearly" flat. Thus the tangent vector V is introduced as a directional derivative operator. The components of such a vector may be denoted as

$$V^\mu(f) = V^\mu \frac{\partial f}{\partial x^\mu}.$$
(2.1)

The vector V maps functions $f \in C^\infty(M, \mathbb{R})$ to $\mathbb{R}$. With a fixed point $p \in M$, it defines the tangent vector space V_p. Introducing the dual space V_p^* and the dual dual space $V_p^{**} \cong V_p$ yields to the definition of tensors as a multilinear map from vectors and dual vectors into numbers [71].

2.1.2 Covariant Derivation Operator

As for two points $p, q \in M$, the tangent spaces V_p and V_q can not directly be compared: Defining for the vector V^μ a traditional derivative

$$\frac{\partial V^\mu}{\partial x^\nu} = \lim_{h \to 0} \frac{V^\mu(x^1, \ldots, x^\nu + h^\nu, \ldots, x^n) - V^\mu(x^1, \ldots, x^\nu + h^\nu, \ldots, x^n)}{h^\nu}$$
(2.2)

fails as even x and $x + h$ may not be compared directly. As a solution, we derive a covariant derivation operator by means of the parallel transport. This operator ∇ will transform like a tensor.

While Wald [71, p. 31] designates requirements for the covariant derivation (linearity, Leibnitz rule, index contraction commutativity, consistency with the index free notation and vanishing torsion tensor/commutativity) and derives the existence of a *connection coefficient* Γ_{bc}^a, one can also introduce the

connection coefficient as the link in the paralle transport which shall be the "correct" way to denote the derivative (2.2), as done in [39]:

$$V^\mu(x \to x + h) := V^\mu(x) - V^\lambda(x)\Gamma^\mu_{\nu\lambda}h^\nu. \tag{2.3}$$

By replacing the traditional difference $V^\mu(x) - V^\mu(x + h)$ by $V^\mu(x) - V^\mu(x \to x + h)$ in equation (2.2), we immediately end up with the definition of the covariant derivative

$$\nabla_\mu V^\nu = \partial_\mu V^\nu + \Gamma^\nu_{\mu\sigma}V^\sigma. \tag{2.4}$$

The covariant derivative naturally extends when computing derivatives of tensors of arbitrary rank. For a (k, l)-Tensor T the derivative is given by

$$\nabla_\alpha T^{\lambda_1...\lambda_k}_{\mu_1...\mu_l} = \partial_\alpha T^{\lambda_1...\lambda_k}_{\mu_1...\mu_l} + \sum_{i=1}^{k} \Gamma^{\lambda_i}_{\alpha\beta} T^{\lambda_1...\beta...\lambda_k}_{\mu_1...\mu_l} - \sum_{j=1}^{l} \Gamma^{\beta}_{\alpha\mu_i} T^{\lambda_1...\lambda_k}_{\mu_1...\beta...\mu_l}. \tag{2.5}$$

2.1.3   The Metric

The connection symbol $\Gamma^\alpha_{\beta\gamma}$ introduced in equation (2.3) is still ambigous. As soon as one equippes the manifold with a metric $g_{\mu\nu}$, there is a special choice, constrained by the requirement that scalars like the inner product of two vectors shall be invariant under parallel transport $t^\alpha\nabla_\alpha$. Mathematically, following [71], for any t, v, w

$$0 \stackrel{!}{=} t^\alpha\nabla_\alpha(g_{\beta\gamma}v^\beta w^\gamma) \quad \Rightarrow \quad 0 = \nabla_\alpha g_{\beta\gamma}. \tag{2.6}$$

This uniquely determined choice of connection symbols is called *Christoffel symbols*. They allow computing the parallel transport and the covariant derivative from the metric:

$$\Gamma^\delta_{\alpha\beta} = \frac{1}{2}g^{\delta\gamma}(\partial_\alpha g_{\beta\delta} + \partial_\beta g_{\alpha\delta} + \partial_\gamma g_{\alpha\beta}) \tag{2.7}$$

2.1.4   Curvature

It is important to remember that for a manifold M there exist different choices of coordinate systems, and only if one found flat space coordinates that are applicable everywhere (that is, $\Gamma = 0$ for all $p \in M$), the manifold is not curved. This reasoning does not work the other way, as the example of choosing polar coordinates in flat space show: There, $\Gamma \neq 0$, but the space is still flat.

In favour to get a measure for spacetime curvature, we can analyse the "defects" of parallel transport around a closed loop with infinitesimal extend. We will see that the change is described by a $(1, 3)$-curvature tensor that will be called *Riemann curvature tensor*.
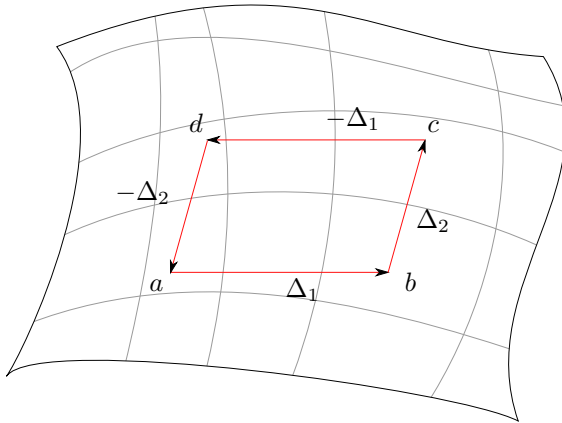

Figure 2.1: Illustration of the closed loop parallel transport on infinitesimal linear displacements Δ^μ_i. When performing the calculation in equatio 2.8, on curved spacetimes one finds a defect which turns out to be the Riemann tensor. In the illustration, for better understanding there is no defect, altought the space-time is heavily curved.

In our setup, we will move the vector V^μ around the closed path $a \to b \to c \to d$ with infinitesimal spacings $+\Delta_1^\mu, +\Delta_2^\mu, -\Delta_1^\mu, -\Delta_2^\mu$. We determine the missing part $\#$ when coming back to a:

$$V^\mu(a) = V^\mu(a) \tag{2.8a}$$

$$V^\mu(b) = V^\mu(a \to a + \Delta_1) = V^\mu(a) - V^\alpha(a)\Gamma^\mu_{\beta\alpha}(a)\Delta_1^\beta \tag{2.8b}$$

$$V^\mu(c) = V^\mu(b \to b + \Delta_2) = V^\mu(b) - V^\gamma(b)\Gamma^\mu_{\delta\gamma}(b)\Delta_2^\delta \tag{2.8c}$$

$$V^\mu(d) = V^\mu(c \to c - \Delta_1) = V^\mu(c) - V^\epsilon(c)\Gamma^\mu_{\kappa\epsilon}(c)(-\Delta_1^\kappa) \tag{2.8d}$$

$$\#V^\mu(a) = V^\mu(d \to d - \Delta_2) = V^\mu(d) - V^\lambda(d)\Gamma^\mu_{\omega\lambda}(d)(-\Delta_2^\omega) \tag{2.8e}$$

Recursively inserting all equations into each other gives a long expression where all linear terms $\mathcal{O}(\Delta_i^\nu)$ vanish, whereas we ignore all third powers $\mathcal{O}(\Delta_i^\nu \Delta_j^\xi \Delta_k^\rho)$. The indices can be relabeled so that the final expression is propertional to second order terms $\mathcal{O}(\Delta_1^\gamma \Delta_2^\delta)$. Note that the christoffel symbols are dependent on the point where they are evaluated. They can be simply moved e.g. at the first insertion step 2.8b into 2.8c by $\Gamma(b) = \Gamma(a) + \partial_\nu \Delta_1^\nu \Gamma(a)$. We end up with

$$\#V^\mu(a) = V^\mu(a)\Big(\underbrace{\partial_\beta\Gamma^\mu_{\gamma\alpha} - \partial_\gamma\Gamma^\mu_{\beta\alpha} + \Gamma^\delta_{\gamma\alpha}\Gamma^\mu_{\beta\delta} - \Gamma^\delta_{\beta\alpha}\Gamma^\mu_{\gamma\delta}}_{R^\mu_{\alpha\beta\gamma}} \Big)\Delta_1^\gamma\Delta_2^\delta \tag{2.9}$$

In the limit, this defines the Riemann tensor $R^\mu_{\alpha\beta\gamma}$.

By tensor contraction, we can define the simpler Ricci tensor $R_{\mu\nu} = R^\lambda_{\mu\lambda\mu}$ and finally the Ricci scalar $R = R^\lambda_\lambda$. This quantity is also called scalar curvature and is the simplest invariant that gives information about flatness of space: As soon as $R = 0$ everywhere, the space is flat.

2.1.5 Einstein Field Equations

With the *Strong principle of equivalence* and the *principle of general covariance* as ingredients, we will derive Einstein equations from a variational principle on the Action $\delta S = 0$ (Hamiltonian principle). Actually, there exist a bunch of other derivations, which e.g derive the Einstein tensor $G_{\mu\nu}$ seperately, with the Ansatz $G_{\mu\nu} = \kappa T_{\mu\nu}$ (as in [25]).

Here, the Ansatz will be the action action, defined by the Lagrangian $\mathcal{L} = \mathcal{L}_G + \mathcal{L}_M$, that is, the interaction (gravitational) part and the source (matter) part. Those two parts are guessed, and basically taking the curvature scalar R and the trace of the energy density tensor $T = T^\lambda_\lambda$ appears to be both an intuitive and good choice. The low energy matching is traditionally accomplished by a prefactor κ, so we end with the *Einstein-Hilbert-Action* including matter,

$$S = \int \sqrt{-g}\, \mathrm{d}^4x \left(\frac{R}{2\kappa} + T \right) \tag{2.10}$$

Note that $\sqrt{-g}$, with g the determinant of the metric $g^{\mu\nu}$, is neccessary for the invariant volume element.

We split up the integral into two parts S_R and S_T and calculate the variation individually:

$$\delta S_R = \frac{1}{2\kappa}\delta \int \sqrt{-g}\, \mathrm{d}^4x\, R_{\mu\nu}g^{\mu\nu} = \frac{1}{2\kappa}\int \mathrm{d}^4x\, R_{\mu\nu}(\delta\sqrt{-g}g^{\mu\nu}) + \frac{1}{2\kappa}\int \mathrm{d}^4x\, \sqrt{-g}g^{\mu\nu}(\delta R_{\mu\nu}) \tag{2.11}$$

One can show that the integral over the variation of $\delta R_{\mu\nu}$ vanishes (surface integral) while the variation $\delta\sqrt{-g}g^{\mu\nu}$ contributes.

Magic happens, the unicorn comes (look it up at [43] and [71] or Weinberg) and we end with

$$\delta S_R = \int \mathrm{d}^4x R_{\mu\nu}(\delta\sqrt{-g}g^{\mu\nu}) = \int \mathrm{d}^4x\sqrt{-g}\left(R_{\mu\nu} - \frac{1}{2}g_{\mu\nu}R \right)\delta g^{\mu\nu}. \tag{2.12}$$

On the other hand, it is

$$\delta S_T = \int \mathrm{d}^4x\, \sqrt{-g}\frac{1}{2}T_{\mu\nu}\delta g^{\mu\nu}. \tag{2.13}$$

By requiring $\delta_S = \delta S_R + \delta S_T = 0$, we immediately read

$$R_{\mu\nu} - \frac{1}{2}g_{\mu\nu}R = \kappa T_{\mu\nu}, \tag{2.14}$$

the *Einstein Field Equations* (EFE). The low energy matching with the Newtonian potential $\Phi = -GM/r$ allows determining $\kappa = -8\pi G$.

The asonishing fact of the Einstein field equations is that they allow deriving all classical predictions of mechanics. The energy conservation law $\nabla_\mu T^{\mu\nu} = 0$ is also intrinsically contained in the Einstein field equations. One can show that in $d = 3 + 1$ space-time dimensions, the EFE are 10 independent non-linear coupled equations which are hard and almost impossible to solve analytically. There are books collecting exact solutions of Einstein gravity like Griffiths [30]. In the next sections, we will discuss the basic solutions of Einstein gravity which are most important in this thesis: The Schwarzschild space-time as well as (Anti-)DeSitter space-times.

2.2 Exact solutions of General Relativity

It is hard to find exact (in terms of analytic) solutions for general relativity, and actually only possible for highly symmetric problems. There are books collecting and classifying exact solutions of general relativity, like Griffiths [30] or Stephani [64]. For an introductory overview about the spacetimes developed by Schwarzschild and DeSitter which are presented in this section, Griffiths text book [30] gives the best overview, and this section follows the reasoning of Griffiths.

In this section, I won't give derivations of the metrics from Einstein equations. Actually, most is covered by the derivation of a quasi-classical source term in section 3.5.

2.2.1 Minkowski space-time

This section is for fixing the notation used in the thesis. Minkowski spacetime (the flat space) is the Einstein solution of the empty space $R_{\mu\nu} = 0$. Working in cartesian coordinates and considering flat space with a $g_{\mu\nu} = \eta_{\mu\nu} = \text{diag}(-1, +1, +1, +1)$ signature, the Minkowski line element can be given as

$$\mathrm{d}s^2 = g_{\mu\nu}\mathrm{d}x^\mu\mathrm{d}x^\nu = -\mathrm{d}t^2 + \mathrm{d}x^2 + \mathrm{d}y^2 + \mathrm{d}z^2, \tag{2.15}$$

with the coordinates $t, x, y, z \in (-\infty, \infty)$. Since we are dealing with high symmetry space times in this thesis, we will most likely work in spherical coordinates, given by the transformation $x = r\sin\theta$, $y = r\sin\theta\sin\phi$ and $z = r\cos\theta$, with $r \in [0, \infty)$, $\theta \in [0, \pi]$ and $\phi \in [0, 2\pi)$ so

$$\mathrm{d}s^2 = -\mathrm{d}t^2 + \mathrm{d}r^2 + r^2(\mathrm{d}\theta^2 + \sin^2\theta\mathrm{d}\phi^2) = -\mathrm{d}t^2 + \mathrm{d}r^2 + r^2\mathrm{d}\Omega_2^2. \tag{2.16}$$

Considering spherical coordinates in the flat Minkowski space is a good learning exercise about *coordinate singularities*: Apparently, the spherical line element (2.16) exhibits singularities at points where $r = 0$, $\sin\theta = 0$ or $r \to \infty$. But the cartesian coordinate choice (2.15) tells us these singularities are not true, or more precisely, in (2.15) we found coordinates without singularities, so the apparent singularities are no true singularities. In contrast, a *curvature singularity* is distinguished by a diverging curvature scalar $R = R_\mu^\mu$. In the next section, we encounter the most simple space-time exposing a curvature singularity.

Ggf. hier noch kurz über Conformal structure sprechen, also Penrose-Diagramme.

2.2.2 Schwarzschild metric

The Schwarzschild metric is the solution for the spherically symmetric static point mass distribution

$$\rho_\theta(r) := \frac{M}{4\pi r^2}\delta(r), \tag{2.17}$$

which is, having electrostatics in mind, the most basic distribution one can imagine.

The Schwarzschild problem, as can be found in text books [43, 71], is typically divided into the *outer* Schwarzschild metric, which describes the space outside a spherically symmetric static mass distribution where $R_{\mu\nu} = 0$, and the *interior* Schwarzschild metric that describes the space-time inside a perfect fluid. It is worth mentioning that we derive the outer Schwarzschild metric from $\rho_\theta(r)$, as given in (2.17), but claim it to be the solution for any $\rho(r)$. This is a consequence of the *Birkhoff theorem* which states that any spherically symmetric solution of the vacuum Einstein field equations must be static and *asymptotically* flat (Minkowski for $r \to \infty$). Note that the Birkhoff theorem only holds in $d = 4$ space-time dimensions (c.f. the next section about higher dimensional gravity).

The solution of (2.17) is given by the Schwarzschild metric

$$\mathrm{d}r^2 = (1 - 2\Phi(r))\mathrm{d}t^2 - (1 - 2\Phi(r))^{-1}\mathrm{d}t^2 - r^2\mathrm{d}\theta^2 - r^2\sin^2(\theta)\mathrm{d}\phi^2 \tag{2.18}$$

with the gravitational potential (Newton's potential) $\Phi(r) = GM/r$. Note that r is not the *distance* of the origin $r = 0$, as space time is deformed and r actually gets timelike for $r < 2GM$.

The radius $r_0 = 2GM$ has a special meaning. At r_0, the metric (2.18) has a *coordinate* singularity which is not a curvature singularity, as one can see when switching e.g. to Eddington-Finkelstein coordinates (Tortoise coordinates). What physically happens at r_0 is that light from the space time region enclosed by the $r = r_0$ cannot escape that surface, it is literally trapped (*trapping* surface or trapped surfaces). For this reason, we call this a *black hole* with event horizon radius r_0, as no event that takes place inside the horizon can be seen by an outside observer.

Actually, the Schwarzschild space-time features a curvature singularity at $r = 0$, this was already "announced" by the dirac delta function, $\rho_\theta(r) \xrightarrow{r \to 0} \infty$. The singularity is shielded by the event horizon, so whatever happens near it cannot be observed outside. In 1969, Roger Penrose formulated the *cosmic censorship hypothesis* which states that curvature singularities are always "hidden" behind an event horizon, so there are no *nacked singularities*. In fact, there are solutions of the EFEs with nacked singularities. We will meet them in this thesis.

Many modifications of the Schwarzschild line element have been investigated, e.g. $g_{00} = 1 - 2GM/r \to \epsilon - 2GM/r$, or by allowing $M \to M(\mathbf{x})$, or by including new physics (like electrical charge). Such approaches have been studied [30], and actually $M \to M(r)$ in a way $\delta \to h(r)$ with $h(r)$ a finite delta approximation describes best the roadmap for this thesis. However, in a general relativity text book, the Schwarzschild metric is primarily extended with angular momentum J and/or electric charge Q, as there exist the old and well-known solutions of the Reissner-Nordström (RN) metric ($Q > 0, J = 0$), the Kerr metric ($Q = 0, J > 0$) and the Kerr-Newman metric ($Q, J > 0$). The *No-hair theorem*, formulated by John Wheeler, postulates that all black hole solutions resulting from the Einstein equations (including electromagnetism, so strictly spoken Einstein-Maxwell equations) are fully characterized by only mass M, electrical charge Q and angular momentum J. Actually, this theorem has not been proven and is therefore only a *conjecture* we will adress in section 3.1 again.

While angular momentum is probably the most relevant one for astronomical purpose, for this thesis it turns out that the RN metric possesses analogons to the regular black hole solutions that will be derived. Therefore, we will face and discuss the RN black holes in section **??**. It may be noted that in this thesis, spinning black holes are not treated. This is not neccessarily bad, since we concentrate on final evaporation phases of black holes. In section 3.1 we will learn more about that.

2.2.3   DeSitter space-time

Expect the flat Minkowski space time, there are also two (unique) solutions with constant curvature R, which can be derived by the 10 isometries of space-time in four dimensional space-time by the local condition [30]

$$R_{\alpha\beta\gamma\delta} = \frac{R}{12}(g_{\alpha\gamma}g_{\beta\delta} - g_{\alpha\delta}g_{\beta\gamma}). \tag{2.19}$$

It can be shown that these two solutions are real vacuum solutions ($T_{\mu\nu} = 0$). For derivation, one takes the Einstein field equations including the cosmological constant Λ and derives $R = 4\Lambda$ as wel as $R_{\alpha\beta} = \Lambda g_{\alpha\beta}$. Space with $R > 0$ is called *de Sitter* space-time (dS) while space with $R < 0$ is called *anti-de Sitter* space-time (AdS), after the dutch physican Willem de Sitter.

There is a set of spherical coordinates that does not cover the complete deSitter space time, but is well enough for the considerations done in this thesis. Robert Mayers calls these the "static patch" coordinates [47]:

$$V(r) = \frac{\Lambda}{3}r^2 := \left(\frac{r}{\ell}\right)^2. \tag{2.20}$$

In deSitter space, our coordinates $g_{00} = 1 - r^2/\ell^2$ expose a singularity at $r_0 = \ell = \sqrt{3/\Lambda}$. Of course, since $R = 4\Lambda > 0$ everywhere, there is no curvature singularity, but the surface $r = \ell$ forms an horizon, anyway: One can derive that this is a *cosmological horizon* [30] which reveals that the universe expansion speed is higher than the speed of light and events beyond $r > \ell$ cannot reach the observer at $r = 0$ anymore. An exact discussion requires introduction of Friedmann-Lemaître-Robertson-Walker-like (FLRW) coordinates and struggling with cosmology, which is beyond the scope of this thesis.

The Anti deSitter spacetime does not possess such horizon. In this thesis, we won't get in touch with the AdS metric any more, but with the dS metric when dealing with regular black hole cores in section 4.4.

(entfernen:) The de Sitter space-time can be extended to the extra dimensions scenario, e.g. done in the famous work by Witten in 1998 [23, 73]. He showed it posses an entropy (in n extra dimensions)

$$S = \frac{r_+^{n+1}\Omega_{n+2}}{4G_N} \tag{2.21}$$

which is propertional to the volume of the Black Hole. Actually this is for the AdS BH.

2.3 Higher dimensional Gravity

From the general relativity viewpoint, in terms of tensor calculus, the generalization from $4 \to d$ space-time dimensions is trivial: We write the Einstein equations in d space-time dimensions as

$$R_{MN} - \frac{1}{2}g_{MN}R = -8\pi G T_{MN} \tag{2.22}$$

with capital latin indices (like A, B, M, N) running e.g. from $0, 1, \ldots d-1$ while the lower greek indices (like α, β, μ, ν) indicing the 4d submanifold from $0 \to 3$ and the lower latin indices (like a, b, m, n) indicing the 3d spatial submanifold as before from $1 \to 3$.

In this section, we will discuss *why* research on higher dimensional gravity was made. This will lead to the higher dimensional black hole in section 1.4.

2.3.1 Kaluza Klein theory

Extending gravity for higher dimensions has a long standing history, first suggestions go back to Nordström and Kaluza [29] and propose using extra dimensions for unification of gravity and electromagnetism. In 1921, this lead to Kalza Klein theory, where Kaluza introduced one space like extradimension (and a scalar field ϕ) that was capable of producing both Einsteins equations and Maxwell equations at once. This works with any four dimensional metric $g_{\mu\nu}$ which is put in the five dimensional extension according to

$$g_{MN} = \begin{bmatrix} g_{\mu\nu}e^{\phi/\sqrt{3}} + e^{-\phi^2}A_\mu A_\nu & e^{-\phi^2}A_\nu \\ e^{-\phi^2}A_\mu & e^{-\phi^2} \end{bmatrix}. \tag{2.23}$$

The Einstein field equations (2.22) for $d = 5$ are a system of 25 equations that decouble to the ordinary 4d Einstein equations with a modified (effective) 4d energy momentum tensor $\tilde{T}_{\mu\nu}$,

$$R_{\mu\nu} - \frac{1}{2}g_{\mu\nu}R = -8\pi G\tilde{T}_{\mu\nu}, \quad \text{with } \tilde{T}_{\mu\nu} = \frac{1}{4}e^{-\sqrt{3}\phi}F_{\mu\sigma}F_\nu^\sigma + \frac{\partial_\mu\phi\partial_\nu\phi}{2}, \tag{2.24}$$

the Maxwell's equations for the field A_μ,

$$\partial_\mu\partial^\nu A^\mu - \partial_\mu\partial^\mu A^\nu = 0 \tag{2.25}$$

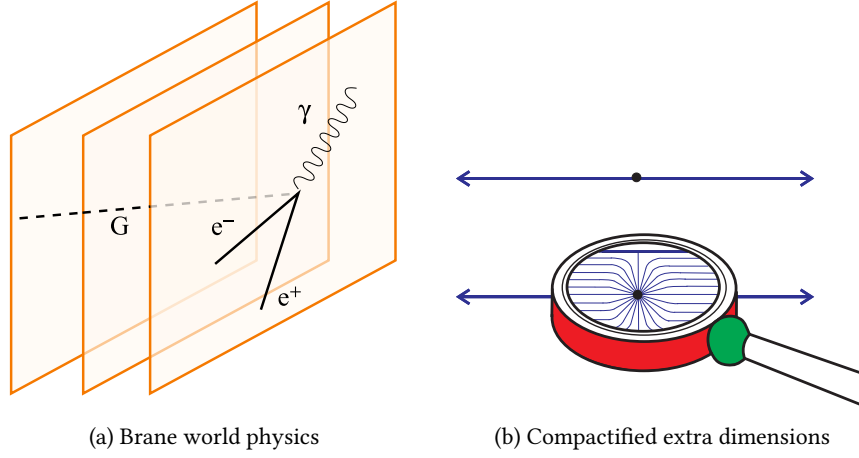(a) Brane world physics (b) Compactified extra dimensions

Figure 2.2: Illustrations how to imagine large extra dimensions and brane world physics. The (orange) 4d branes are displayed as 2d surfaces, while one extra dimension is displayed horizontally. While the QED process takes place on the brane, and neither electron, positron and photon can escape the brane, the graviton is supposed to freely traverse the whole space-time.

The compactification picture shows where one faces extra dimensions even in real life: When zooming in, the one dimensional horizontal line shows a vertical substructure.

and a relativistic equation for the scalar field ϕ

$$\partial_\mu \partial^\mu \phi = \frac{-\sqrt{3}}{4} e^{-\sqrt{\phi}} F_{\mu\nu} F^{\mu\nu}. \tag{2.26}$$

Note that in this theory, the gravitational coupling constant G was untouched.

2.3.2 Randall-Sundrum scenario

The Randall-Sundrum (RS) model was proposed in 1999 and persists of the existence of one large spatial extra dimension with negative curvature (AdS). The five dimensional line element is given by [35]

$$ds^2 = e^{-2kr_c|y|} g_{\mu\nu} dx^\mu dx^\nu + r_c^2 dy \tag{2.27}$$

with $g_{\mu\nu}$ the 4d space time, $k \sim 1/L_*^2$ a parameter of the order of the fundamental planck scale, y the extra coordinate and r_c the compactification radius of the extra dimension. The RS metric can be derived like KK from the 5d EFEs with negative cosmological constant, and thus the bulk is interpreted as a slice in the 5d AdS space.

2.3.3 ADD-model and Large extra dimensions

In 1998, Nima Arkani-Hamed, Savas Dimopoulos and Gia Dvali (ADD) proposed a model with n large spatial extra dimensions (LXDs or LEDs). In this model, we live in a $d = 4 + n$ dimensional space-time. The observable four-dimensional universe is called the *brane* (the term comes from membrane), embedded in the higher-dimensional *bulk* space-time. These n extra dimensions are considered flat and compactified, like the extra dimension in the KK theory, but the compactification radius R_c is considered *large* compared to the Planck length. Typical values are $R_c \approx 1$mm. This value is small enough to agree with non-observed deviations from Newton's law. The idea of the ADD model is, that all Standard model fields *live* on the brane, that is, do not notice the existence of more than four dimensions, while the gravitational field is allowed to propagate everywhere (bulk and brane). Figure 2.2 illustrates possible ways to imagine brane and bulk space, and compactified extra dimensions.

The large extra dimension scenario can solve the weak hierarchy problem of the Standard model by imposing a new fundamental mass scale M_* which produces the observable 4d Planck mass scale M_{Pl} by

integrating out the volume of the extra dimensions. The weak hierarchy problem is the strange fact that the electro-weak energy scale (masses of electro-weak gauge bosons) is about 10^{32} times smaller than the gravity energy scale (Planck mass). In other formulations, it is the question why the Higgs boson is so much lighter than M_{Pl}. The extra dimensional outcome states that we see only an effective weak coupling constant $G = 1/M_{\mathrm{Pl}}^2$ because it is the result of the integrated out volume of the extra dimensions, where gravity also propagates. We define this ratio according as

$$M_{\mathrm{Pl}}^2 = C_n V_n M_*^{n+2} \tag{2.28}$$

with V_n the volume of the enrolled extra dimensions, with tori and compactification radii R_c e.g. $V_n = (2\pi R_c)^n$ and a dimensionless prefactor $C_n = \mathcal{O}(1)$.

Note that there are multiple conventions about the prefactor C_n in (2.28). My convention is most like the Han-Lykken-Zhang notation (HLZ), as proposed in the appendix of [15]:

$$C_n = \left(\frac{\Omega_{n+2}}{8\pi} \right)^{\frac{1}{n+2}} \tag{2.29}$$

The prefactor is neccessary to match the 4d Newton's potential. In my convention, $C_0 = {}^1\!/_2$ and therefore $M_{\mathrm{Pl}} = {}^1\!/_2 M_*$. Das ist so noch nicht wirklich richtig, here should be at least one more 2 to ensure $M_{\mathrm{Pl}} = M_*$.

In the ADD scenario, these extra dimensions were to be meant *large* in extend, that is, in the milimeter scale. Thus, the fundamental couping reaches the TeV scale even with one extra dimension. This opens the door for experimental tests, as the center of mass energy of the Large Hadron Collider (LHC) at cern is in the same order of magnitude (10 TeV).

2.3.4 Black Holes in particle detectors

There are lot of good and lengthy reviews, e.g. by Kanti and Winstanley [34, 35]. See e.g. for Black Holes at LHC: Bleicher 2010 [8], Koch [40], von 2013 [51] and the 2014 review [9].

In this terms, we can immediately formulate the natural higher dimensional extension of the Schwarzschild energy density

$$\rho(\mathbf{x}) = \frac{M}{\Omega_{2+n} r^{2+n}} \delta^{1+n}(\mathbf{x}), \tag{2.30}$$

making use of the higher dimensional delta function δ^d and the surface Ω_{2+n}. This gives the gravitational potential

$$V(r) = \frac{2}{n+2} \frac{M}{M_*^{2+n}} \frac{1}{r^{1+n}}. \tag{2.31}$$

for the *Schwarzschild-Tangherlini* metric

$$\mathrm{d}s^2 = (1 - V(r))\mathrm{d}t^2 - (1 - V(r))^{-1}\mathrm{d}r^2 + r^{2+n}\mathrm{d}\Omega_{2+n}^2. \tag{2.32}$$

Chapter 3

Short-scale improved Black Holes

In this section, I want to emphazise the breakdown of general relativity at quantum scales (the Planck scale) and give an overview about theories trying to cure the ultra violet behaviour. We then formulate requirements for a final state spherically symmetric UV improved model and derive a metric which fulfills the requirements.

3.1   Black hole evaporation phases

Mini Black holes that can be e.g. produced in particle detectors like discussed in the last section evaporate by Hawking radiation. This process is typically categorized in four phases [9, 40]:

- **Balding phase**. In this phase the black hole looses the *hair* which consist of assymetries (multipole moments), gauge field hair.

- **Spin down phase**. The black hole radiates away angular momentum and mass.

- **Schwarzschild phase**, where the black hole is spherical and still radiates.

- **Planck phase**, where the black hole mass reaches the Planck mass and quantum gravity effects get strong.
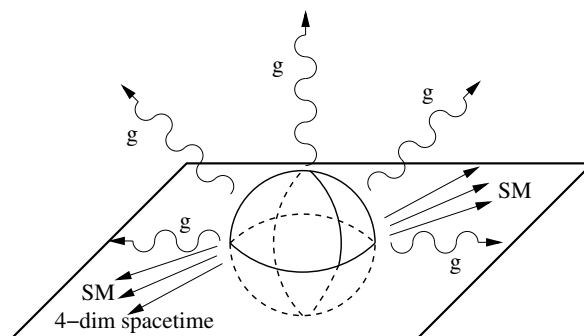

Figure 3.1: Artistic illustration how Hawking evaporation on the brane and bulk can be imagined, taken from the Cavaglia review [15].

3.2 Problems of the Schwarzschild Black Hole

One of the tenets of high energy physics is the association of the failure of a theory at scales where the theory predicts singularitiess. It is common belief that nature is nonsingular in the same way (classical) physics is supposed to be "smooth" everywhere. Against this backdrop, the obvious problem of the Schwarzschild black hole is the curvature singularity in the origin which may be traced to the dirac delta distribution composing the matter source $\delta(\mathbf{x})$. Anyway, the dirac delta may be seen as an idealization, so this may be casted as a philosophical problem.

Actually the real flaws occur at Black Hole thermodynamics. The Hawking temperature for black holes is defined by the surface gravity $\kappa = \partial_r g_{00}|_{r_H}$ by

$$T_H = \frac{\hbar \kappa}{2\pi} = \frac{1}{8\pi GM}. \tag{3.1}$$

Assuming energy loss when a black hole radiates, the evaporating black hole get's hotter and hotter, and the picture breaks down when $T \sim M$, that is, when the emission occurs at a temperature of the order of the black hole mass.

Based on this temperature, the black hole thermodynamics are constructed. The Schwarzschild heat capacity $C_T = dM/dT$ is negative and approaches asymptotically zero for increasing temperatures. Frolov therefore calls Schwarzschild thermodynamics *ill defined*, since such a Black hole cannot be in a stable equilibrium with a surrounding heat bath [26].

Despite the obvious fundamental contradictions between general relativity and quantum mechanics, at shortest scales there is even a tangible particle-black hole *duality*, illustrated in figure (3.2a). On the quantum mechanical side, each particle with mass (=energy) m can be assigned a length scale. This can be the compton wavelength $\lambda_C = \hbar/mc$, so $L_{\text{particle}} \sim 1/m$, as the red curve indicates. On the other hand, the Black hole picture assigns each mass distribution a length by means of the Schwarzschild event horizon $r_H = 2GM/c^2$, so $L_{\text{Black hole}} \sim m$, as the blue curve indicates. These two curves cross at the planck scale $L_{\text{particle}} = L_{\text{Black hole}} = \sqrt{\hbar c/G} := L_{\text{Pl}}$ (numerical factors like the 2 are suppressed in this picture). Let's trace as a Gedankenexperiment a particle in an accelerator where it's energy (velocity) is increased, resulting in a better length scale resolution (particle compression, red arrow). At the planck scale M_{pl}, suddenly the *hoop conjecture* expects the particle to become a black hole, and further (fictive) acceleration increases the size of the object again. Now we turn off the accelerator, and by Hawking evaporation the black hole decays (blue arrow). As there is no *inverse hoop conjecture* in particle physics, nothing prevents the Schwarzschild black hole from evaporating below the planck scale. Suddenly, we end up with a situation where two theories predict two different sizes for the same system. Which one is right?

There are two ways out of this awkward situation: Either the general relativity breaks down and must be replaced by a completely different theory, or it can be saved by some kind of *completeness*. In figure 3.2b we sketched such a solution: By modifying the gravitational event horizon in a way that it smoothly merges into the particle picture, we get a unique particle–black hole interpretation and a *minimum length scale* of physics L_{Pl}. In this theory, there is literally no way to probe distances below L_{Pl} as it is either circumvented by quantum mechanical uncertainity or black hole production.

3.3 Quantum gravity black holes

In this section, I want to give a two-page overview about black holes in different quantum gravity approaches and their relationship to this work. I primarily follow the "six families of black holes" proposed in [55] and append *String theory*, which is certainly the most popular candidate for QG.

Non-local gravity Black Holes

In this category of approaches, the starting point is a nonlocal field theory by means of a nonlocal contribution to the geometric part of the Einstein field equations. In [46], this is done with a derivation operator
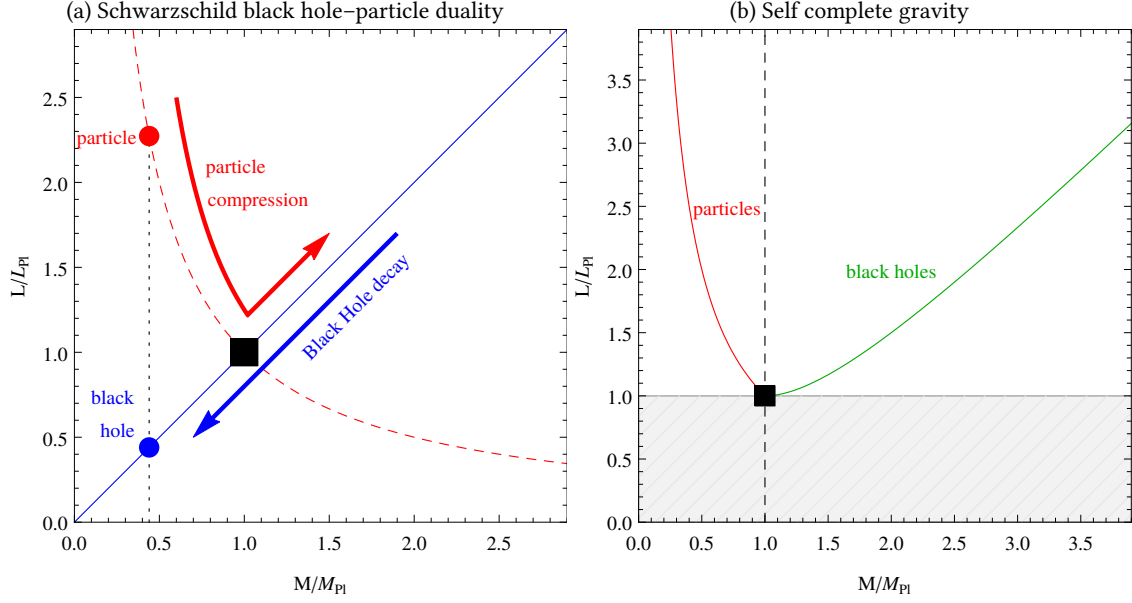
(a) Schwarzschild black hole–particle duality   (b) Self complete gravity

Figure 3.2: Length-vs-Mass pictures

acting on the Einstein tensor in a way that

$$\mathcal{F}^{-2}(\Box(x)/\Lambda_G^2)\left(R_{\mu\nu} - \frac{1}{2}g_{\mu\nu}R\right) = 8\pi G_N T_{\mu\nu}. \tag{3.2}$$

This goes back to nonlocal action modifications in gravity proposed by Barvinsky (see [6] for a recent review from him and [5] for a more comprehensive early work). Actually, such an approach is also used for curing divergences at pertubative expansion of the Einstein-Hilbert action up to a super-renormalizable theory of Quantum Gravity [45].

In the last chapter 6 of this thesis, we also discuss nonlocal operators $\mathcal{F}^{-2}$ in spite of finding a dual theory to a quantum matter density.

Noncommutative Black Holes

Noncommutative geometry suggests a "fuzzy" spacetime by imposing a commutation relation on the quantum-mechanical position operator $\mathbf{x}^\mu$. In terms, this reads

$$[\mathbf{x}^\mu, \mathbf{x}^\nu] = i\theta^{\mu\nu} \tag{3.3}$$

with the matrix $\theta > 0$ imposing the "discretization" of space-time. This idea leads to a space time uncertainty and finally to a gaussian energy density approach as dirac replacement in the noncommutative inspired Schwarzschild solution,

$$\rho_\theta(r) = \frac{M}{(4\pi\theta)^{3/2}}e^{-r^2/4\theta}. \tag{3.4}$$

From this equation one can read that $r \sim \sqrt{\theta}$ corresponds to the length scale where noncommutative effects get strong. Funny enough, the metric produced by (3.4) possesses a regular core like the one we will contrive in this chapter [52].

A long review about Noncommutative Black Holes is [48]. The first extradimensional extension from Rizzo 2005 [60] actually determined the syntax and conventions used in this thesis.

Generalized Uncertainty Principle Black Holes

The generalized uncertainty principle is perhaps the closest approach to create a "matching" picture 3.2b. It can be formulated by suggesting as well a modified compton scale as a generalized event horizon [11,12] and states, in the simplest form

$$\Delta x \Delta p \geq \frac{\hbar}{2} \left(1 + \alpha x^2 + \beta p^2 \right).$$ (3.5)

Note that for $\alpha = \beta = 0$, this is the Heisenberg uncertainty principle. By means of a Hilbert space representation [36], for $\alpha = 0$ on can deduce a nice modified momentum integration measure where $p \sim \sqrt{\beta}$ plays the role of a high energy regulator, and this can be used to compute the GUP-Schwarzschild black hole with energy density [32,33]

$$\rho_\beta(r) = \frac{M}{(2\pi)^3} \int \frac{\mathrm{d}^3 p}{1 + \beta p^2} e^{i\mathbf{x}\cdot\mathbf{P}}.$$ (3.6)

Suprisingly, there also is a link to this thesis: Densities like (3.6) have been extended to higher dimensions [41], and the integration technique to solve nonlocal operators introduced in chapter 6 turned out to be successful also to compute fourier transformations of GUP operators.

Loop Quantum Black Holes

Loop Quantum Gravity (LQG) is the competitor for string theory that has the major advantage of preserving *background-independence*, as this is a major pillar of general relativity. Therefore, LQG cannot be a pertubative expansion of quantum GR by means of $\tilde{g}_{\mu\nu} = g_{\mu\nu} + h_{\mu\nu}$, since this would distinguish a special fixed classical background metric $g_{\mu\nu}$. The main principle in LQG is general covariance paired with quantum principles. Contemporary formulations use a graph as basic principe, a network (the "foam") with spacetime points as vertices and a discrete minimal length distance and therefore refined the building word *loop* QG. According to Asthekar, "loops play no essential role in the theory now, for historical reasons, this name is widely used"; there lies the close relationship to lattice gauge theories, as closed loops resemble Wilson plaquettes [61,70].

It is a long way from loop quantum gravity to loop quantum black holes (LQBHs), and contemporary research about LQBHs is fairly less "descriptive" than the black holes modified by the principled mentioned before. See e.g. Modesto [44] who, amongst other things, finds out after a lengthy calculation that the Schwarzschild curvature singularity is no more present in LQBH.

Let me remark that a particularly significant result is a fundamental explanation of the black hole logarithmic entropy correction that was predicted by Wilson. We will discuss the logarithmic black hole entropy term in depth in section 5.4.

For an paedagogical review about LQG, I enjoyed the texts of Thiemann [68,69] and Ashtekar [2]. For a pedagocigal introduction with focus on spin foams, see [58].

Asymptotically safe gravity Black Holes

Asymptotically safe gravity is built on a running coupling $G(k)$ which is the result of renormalization group treatments; general covariance is maintained with this approach. The basic idea is to make gravity an effective theory at momentum scale k and therefore be safely able to do physics with momenta $k' \gg k$.

Applied to black holes, $G(r)$ takes the place of Newton's contant in the Schwarzschild metric [24]. Thus it is possible to get black hole remnants that resemble the holographic profile we encounter in the next sections.

For introductory papers, see e.g. Reuter [10,59] and the review [56] by the same author.

Black holes in String theory

String theory perhaps fits least in this list, as in String theory, general relativity is literally *replaced* with the more fundamental theory.

String theory is the theory of quantum-mechanical relativistic one-dimensional "vibring strings" (waves), and according to the popular picture, different excitation energies correspond to different point-like particles postulated by the standard model of particle physics. The term "string theory" is usually used similary to superstring theory, that is, string theory including suppersymmetry (SUSY, a symmetry that relates each boson to it's superpartner, the fermion, and vice versa). The existence of extra dimensions, as introduced in section 2.3, is actually predicted by string theory. String theory is most criticised because it's large number of solutions and (new) physical constants and especially because the dependence on a background spacetime which explicitly breaks general covariance. On the other hand, string theory may be treated pertubatively.

Considering black holes, string theory is especially able to make statements about extremal black hole situations, as we will encounter in the next chapter. The enticing recast of an extremal black hole as a *particle* is unique to string theory. String theory also predicts a logarithmic entropy correction as LQG.

String theory is handled e.g. in the book of Kiefer [38], black holes in string theory are discussed in [42]. Probably a good closing overview over all approaches gives the review article [37].

3.4 Requirements for self-complete Black Hole metrics

The following three properties for short-scale improved Black holes were proposed in [53]. They imply the newly developed theory is equipped with a *characteristic length scale* l_0 which is, of course, associated with an energy scale $1/l_0$ of theory validity.

1. A *regular black hole* that has no more curvature (Ricci scalar) singularity at the origin, in terms

$$R(0) < \infty. \tag{3.7}$$

2. *Classical low-energy limit*, that is, Schwarzschild-Behaviour of the metric for big distances, in terms

$$g_{00}(r) = \frac{2GM}{r} \quad \text{for} \quad r \gtrsim l_0. \tag{3.8}$$

3. *Self-encoding* of the characteristic minimal length scale l_0 in the radius of the *extremal* configuration r_0, that is,

$$l_0 = r_0. \tag{3.9}$$

This third requirement is crucial: Self-encoding enables l_0 being the only *universal scale*, as the theory requires no new length scale (parameters).

3.5 Quasi-classical source terms

3.5.1 Derivation of the metric

In this section, I want to derive the metric for a potential $V(r)$ that behaves like the Schwarzschild potential $V(r) = 2GM/r$ at large r. As already stated, my conventions follow [60].

The starting point is a static isotropic matter density $\rho(r)$ with $\lim_{r \to \infty} \rho(r) = 0$. The Ansatz for the solution is the $d = n + 4$ dimensional spherical symmetric and static metric

$$\mathrm{d}s^2 = -e^{\nu(r)}\mathrm{d}t^2 + e^{-\nu(r)}\mathrm{d}r^2 + r^2\mathrm{d}\Omega_{n+2}^2 \tag{3.10}$$

$$= -\left(1 - V(r)\right)\mathrm{d}t^2 + \left(1 - V(r)\right)^{-1}\mathrm{d}r^2 + r^2\mathrm{d}\Omega_{n+2}^2 \tag{3.11}$$

with Ω_{n+2} the surface line element of an $(n+3)$ sphere (for details about the surface sphere, see appendix 6.2.2). The spherical coordinates are given by $x_\mu = (x_0, \vec{x}) = (x_0, r, \phi, \theta_1, \dots, \theta_{n+2})$, but I will write i instead of θ_i ($i = 1, \dots, m$ and $m := n + 2$) in the indices to improve readability, refering to the diagonal coefficients in the metric as

$$g_{AB} = \mathrm{diag}\left(g_{00}(r), -g_{00}^{-1}(r), g_{\phi\phi}(r, \phi), g_{11}(r, \theta_1), \dots, g_{mm}(r, \theta_m)\right) \tag{3.12}$$

The argumentation follows the derivation of the inner Schwarzschild solution, as can be found in General Relativity textbooks: The property $-g_{00} = g_{11}^{-1}$ is required for flat space at large distances.

Given the mattern density and the metric ansatz, the stress tensor T^{NM} can be determined. Due to the symmetry of the problem, it can already be stated as

$$T_N^M = \mathrm{diag}\left(T_0^0, T_r^r, T_\phi^\phi, T_1^1, T_2^2, \dots, T_m^m,\right) = \mathrm{diag}\left(\rho, \rho, p, p, \dots, p\right), \tag{3.13}$$

following [52, 60]. We now switch to $(1, 1)$ tensor form in order to write the conservation of energy equation $\nabla_N T^{NM} = 0$ as $\nabla_N T_M^N = 0$ with

$$T_B^A = g_{BC}T^{AC} = g_{BB}T^{AB} = \mathrm{diag}(g_{00}T^{00}, g_{rr}T^{rr}, \dots, g_{mm}T^{mm}). \tag{3.14}$$

One can see that only the equation with index $M = r$ contributes new information. In order to solve this equation (no sum convention here):

$$0 = \nabla_0 T_r^0 + \nabla_r T_r^r + \sum_i \nabla_i T_r^i \tag{3.15}$$

we need to compute the covariant derivatives derivative ∇_N and christoffel symbol Γ_{AB}^C that break down to compact expressions (see appendix 6.2.2 for the definitions):

$$\nabla_0 T_r^0 = \partial_0 T_r^0 + \Gamma_{0D}^0 T_r^D - \Gamma_{0r}^D T_D^0 = \frac{1}{2} g^{00} T_r^r \partial_r g_{tt} + \frac{1}{2} g^{00} T_0^0 \partial_r g_{tt} \tag{3.16a}$$

$$\nabla_r T_r^r = \partial_r T_r^r + \Gamma_{rD}^r T_r^D - \Gamma_{rr}^D T_D^r = \partial_r T_r^r \tag{3.16b}$$

$$\forall i : \quad \nabla_i T_r^i = \partial_i T_r^i + \Gamma_{iD}^i T_r^D - \Gamma_{0r}^D T_D^i = \frac{1}{2} g^{ii} T_r^r \partial_r g_{ii} + \frac{1}{2} g^{ii} T_0^0 \partial_r g_{ii} \tag{3.16c}$$

We end up with the explicit equation

$$0 = \partial_r T_r^r + \frac{1}{2} g^{00} \left(T_r^r - T_0^0 \right) \partial_r g_{00} + \frac{1}{2} \sum_i g^{ii} \left(T_r^r - T_i^i \right) \partial_r g_{ii} \tag{3.17}$$

Now plugging in the Ansatz for T_B^A, the term $\left(T_r^r - T_0^0 \right)$ vanishes. For all angles, the term

$$g^{ii} \partial_r g_{ii} = \frac{1}{r^2 \sin^j(\theta_j)} \partial_r \left(r^2 \sin^j(\theta_j) \right) = \frac{2}{r} \tag{3.18}$$

is the same and thus all remaining energy momentum components are determined to

$$T_i^i = T_0^0 + \frac{r}{n+2} \partial_r T_0^0 = \rho + \frac{r}{n+2} \partial_r \rho. \tag{3.19}$$

In order to solve the Einstein equation, in addition to the energy momentum tensor we need the Ricci tensor as additional ingredient. It is given as the contraction of the Riemann tensor

$$R_{\mu\nu} = \partial_\lambda \Gamma_{\nu\mu}^\lambda - \partial_\nu \Gamma_{\lambda\mu}^\lambda + \Gamma_{\mu\gamma}^\lambda \Gamma_{\nu\mu}^\gamma - \Gamma_{\nu\gamma}^\lambda \Gamma_{\lambda\mu}^\gamma, \tag{3.20}$$

see Appendix 6.2.2 for the values of all Christoffel symbols. The Ricci tensor is again diagonal, with the entries

$$R_0^0 = R_r^r = -\frac{e^\nu}{2} \left(\partial_r^2 \nu + (\partial_r \nu)^2 + (n+2) \frac{\partial_r \nu}{r} \right) = \frac{1}{2} V''(r) - \frac{n+2}{2} \frac{V'(r)}{r} \tag{3.21a}$$

$$\forall i : \quad R_i^i = \frac{1 + n - e^\nu (1 + n + r \partial_r \nu)}{r^2} = (1+n) \frac{V(r)}{r^2} + \frac{V'(r)}{r}. \tag{3.21b}$$

The Ricci scalar is then given by

$$R = R_N^N = \frac{(n+2)V(r)}{r^2} + V''(r) \tag{3.22}$$

Now we can write out the Einstein equations $G_{\mu\nu} = R_{\mu\nu} - \frac{1}{2} R g_{\mu\nu}$ in a trace reversed form, in $(1,1)$ tensor notation for d dimensions:

$$R_A^B = \frac{1}{M_*^{n+2}} \left(T_A^B - \delta_A^B \frac{T_C^C}{n+2} \right) \tag{3.23}$$

Since R, T, δ are diagonal, the Einstein equations reduce to d non-zero equations where finally only two equations differ from each other, identified by their indexes $A, B = r, r$ and $A, B = i, i$. The later one gives the following first order differential equation for $V(r)$:

$$V'(r) + \frac{n+1}{r} V(r) = \frac{1}{M_*^{n+2}} \frac{2r\rho(r)}{n+2} \tag{3.24}$$

The general solution of the metric for any $\rho(r)$ is given by the integral

$$V(r) = \frac{1}{r^{n+1}} \left(\frac{2}{(n+2)M_*^{n+2}} \int\limits_{c_1}^r x^{n+2} \rho(x) \mathrm{d}x + c_2 \right) \quad \text{with} \quad c_1, c_2 = \text{const} \tag{3.25}$$

The boundary values $V(0)$ and $V'(0)$ give rise to the two integration contants c_1 and c_2. Physically, they allow the low-energy matching of the theory. In our context, c_1 is important for discussion about minimal lengths.

(a) Holographic profile $h(r)$ in different LXDs n (b) Self-encoding profile $h_\alpha(r)$ in $n = 2$ for different α
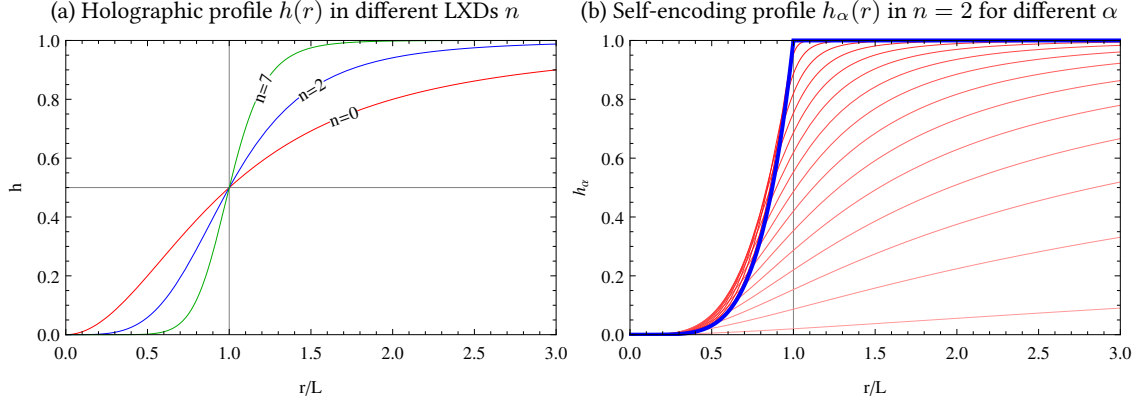
Figure 3.3: The two chosen Heaviside step function smearing functions with their characteristic behaviour, each scaled against their built in length scales $\tilde{r}_0$. For more details see Appendix 6.2.2.

3.5.2 Smeared matter density

Starting with the Schwarzschild-Tangherlini point-like static and spherically symmetric density

$$\rho(r) = \frac{M}{\Omega_{n+2} \, r^{n+2}} \delta(r) \tag{3.26}$$

we replace the Dirac delta $\rho(r)$ by a smeared version which we define as the derivative $\frac{\mathrm{d}\Theta(r)}{\mathrm{d}r} = \delta(r)$ of the Heaviside unit step function

$$\Theta(r) = \begin{cases} 0 & \text{when} \quad r < 0 \\ 1 & \quad r \geq 0 \end{cases}. \tag{3.27}$$

We therefore choose the generic *Schwarzschild-like* energy density

$$\rho(r) = \frac{M}{\Omega_{n+2} \, r^{n+2}} \frac{\mathrm{d}H(r)}{\mathrm{d}r}. \tag{3.28}$$

which, when inserting into the integral 3.25, gives us the generic metric, for a given $H(r)$, as

$$V(r) = \frac{2}{2+n} \frac{M}{M_*^{n+2}} \frac{H(r)}{r^{n+1}}. \tag{3.29}$$

A closer discussion about the physical meaning of the mass parameter M will be given in section 4.1.

3.6 Choices for mass profiles and their d-dimensional extension

In Nicolini and Spallucci's paper about holographic screens in UV self complete gravity [53], there are two mass profiles presented which I will refer in this work to as

$$\text{the } \textit{self-regular} \text{ profile} \quad h_\alpha(r) = \frac{r^3}{(r^\alpha + \tilde{r}_0^\alpha/2)^{3/\alpha}} \quad \text{and} \tag{3.30a}$$

$$\text{the } \textit{holographic} \text{ profile} \quad h(r) = \frac{r^2}{r^2 + \tilde{r}_0^2}. \tag{3.30b}$$

Each of them builds a matter density and thus a space-time by plugging $H \in \{h_\alpha, h\}$ into

$$\rho(r) = \frac{M}{\Omega_{n+2} \, r^{n+2}} \frac{\mathrm{d}H(r)}{\mathrm{d}r}. \tag{3.28 revisited}$$

Note that these profiles are just invented from nothing, that is, they are an *educated guess* or *ab-initio*, to solve the problems they are confronted with on the next pages. The special feature of the main paper of this thesis [53] is that *there is no further ingredient than general relativity*. We did not stress a more advanced theory like string theory or loop quantum theory to produce the densities (3.28) in the limit. But these profiles do not only produce *toy models* but have profound physical properties that we uncover in the next two chapters. We will also learn about the reason of the naming: While the *self-regular* profile fulfills all requirements 1-3 from section 3.4, especially the regularity, the holographic one is not regular, but features logarithmic corrections to the black hole entropy, as we will see in section 5.4.

3.6.1 Extension to extra dimensions

In this work, I investigate the properties of black holes of the profiles extended to n large extra dimensions. It turns out that the correct choice is

$$h(r) = \frac{r^{2+n}}{r^{2+n} + \tilde{r}_0^{2+n}} \quad \text{and} \quad h_\alpha(r) = \frac{r^{3+n}}{(r^\alpha + \tilde{r}_0^\alpha/2)^{\frac{3+n}{\alpha}}}. \qquad (3.31, 3.32)$$

With $n \to 0$, they reduce to the 4-dimensional models used in [53].

It may be denoted that these choices were "guessed", as every $2 \to 2+n$ or $3 \to 3+n$ in a "natural" manner. The choice for the holographic model is "proven" by yielding the required entropic corrections, as shown in section 5.4. For the self-encoding model, where is the motivation?

3.6.2 Length scales

Before heading to the physical properties of black holes created by such mass profiles, let me shortly sum up the new variables introduced by those profiles: In any case, it is a length scale $\tilde{r}_0$ that plays the role of the *width* of the delta/heaviside approximation, as the variance σ in the well-known Gaussian approximation

$$\delta_\sigma(r) = \frac{1}{\sqrt{2\pi\sigma}} \exp\left(-\frac{r^2}{2\sigma}\right), \quad \delta(r) = \lim_{\sigma \to 0} \delta_\sigma(r). \qquad (3.33)$$

Figure 3.3 displays the two profiles rescaled to their length scale $\tilde{r}_0$. For the holographic profile, $\tilde{r}_0$ is a kind of "half-life scale", as $h(\tilde{r}_0) = 1/2$, for the self-encoding one it is $h_\alpha(\tilde{r}_0) = (3/2)^{-\frac{3+n}{\alpha}}$. Figure 3.3a shows that increasing n create a sharper distribution. As a side note, note that for $n \to \infty$, the curve resembles a displaced step function $h_{n\to\infty}(r) = \Theta(r - \tilde{r}_0)$. This reflects the fact that all volume in a ∞-sphere lives on the surface.

Figure 3.3b looks basically the same in any dimension, but shows how the additional degree of freedom α modifys the distribution. Bigger α create a sharper curve until the limit $\alpha \to \infty$ where the difference between $h(r)$ and $h_\alpha(r)$ clearly stands out: The additional degree of freedom can be used for a $h_\infty(r) \sim r^{3+n}$ behaviour for $r < \tilde{r}_0$ while $h_\infty(r) = 1$ for $r > \tilde{r}_0$.

Note that until now, we have not given $\tilde{r}_0$ and α a physical meaning, they are just mathematical constants. Linking $\tilde{r}_0$ according to the self-encoding principle (3.9) to a physical length scale l_0 is the agenda for the next chapter.

3.6.3 The Schwarschild-limit

In the next sections, I will discuss the properties of the class of $\Theta(r) \to H(r)$ smeared black holes. For comparison, it will frequently be useful to take back the limit $H(r) \to \Theta(r)$. To do so mathematically correct, one examines the limit of the regulator $\tilde{r}_0 \to 0$.. Thus, it will be (only) safe for $r > 0$ to replace any occurrence of

$$H(r) \to 1, H'(r) \to 0, H''(r) \to 0, \dots \qquad (3.34)$$

according to the finite values $\Theta(r) = 1$ and $\delta(r) = 0$ for $r > 0$. This of course also holds for products like $H(r)H'(r) \to 0$. Interestingly, this naive approach is also doable at $r = 0$, but one may not expect this would give statements of divergence behaviour.

Chapter 4

Geometry of the Black Holes

In this chapter, I will discuss the geometry and conformal structure of the family of Black Hole geometries presented in the previous chapter. This will lead to the discussion about the special features of regular black holes.

4.1 The Mass

The mass contained inside a $(3 + n)$-sphere (we will refer to that object by $\mathcal{B}(r)$) with radius r is given by the integral

$$m(r) = \int_{\mathcal{B}(r)} \rho(x) \mathrm{d}^{n+3} x = M \int_0^r H'(r) = M H(r). \tag{4.1}$$

From the physical viewpoint, this is the mass visible to any observer outside this sphere, that is, at position $r' > r$. Note that actually, we make a small mistake, because the correct integral measure would be

$$\int_{\mathcal{B}(r)} \sqrt{-g}\, \mathrm{d}^{n+3} x\, \rho(x), \tag{4.2}$$

but everybody does that.

From the mathematical viewpoint, the mass M is just a constant that may be used to fulfill the horizon equation $V(r) = 1$. Therefore I set

$$M = \frac{n+2}{2} M_*^{n+2} \frac{r_H^{n+1}}{H(r_H)}, \tag{4.3}$$

so when plugging into the metric

$$V(r) = \frac{2}{n+2} \frac{M}{M_*^{n+2}} \frac{H(r)}{r^{n+1}} \tag{3.29 revisited}$$

the horizon equation $V(r) = 1$ is fulfilled at $r = r_H$. The physical meaing of M is the mass of a black hole of radius r_H [54]. When substituting $n + 1$ powers of M_* by $M_* = 1/L_*$, we can easily relate

$$M = \frac{n+2}{2} \left(\frac{r_H}{L_*} \right)^{n+1} \frac{1}{H(r_H)} M_*. \tag{4.4}$$

Todo: ADM Mass

(a) g_{00} for the holographic metric (h).

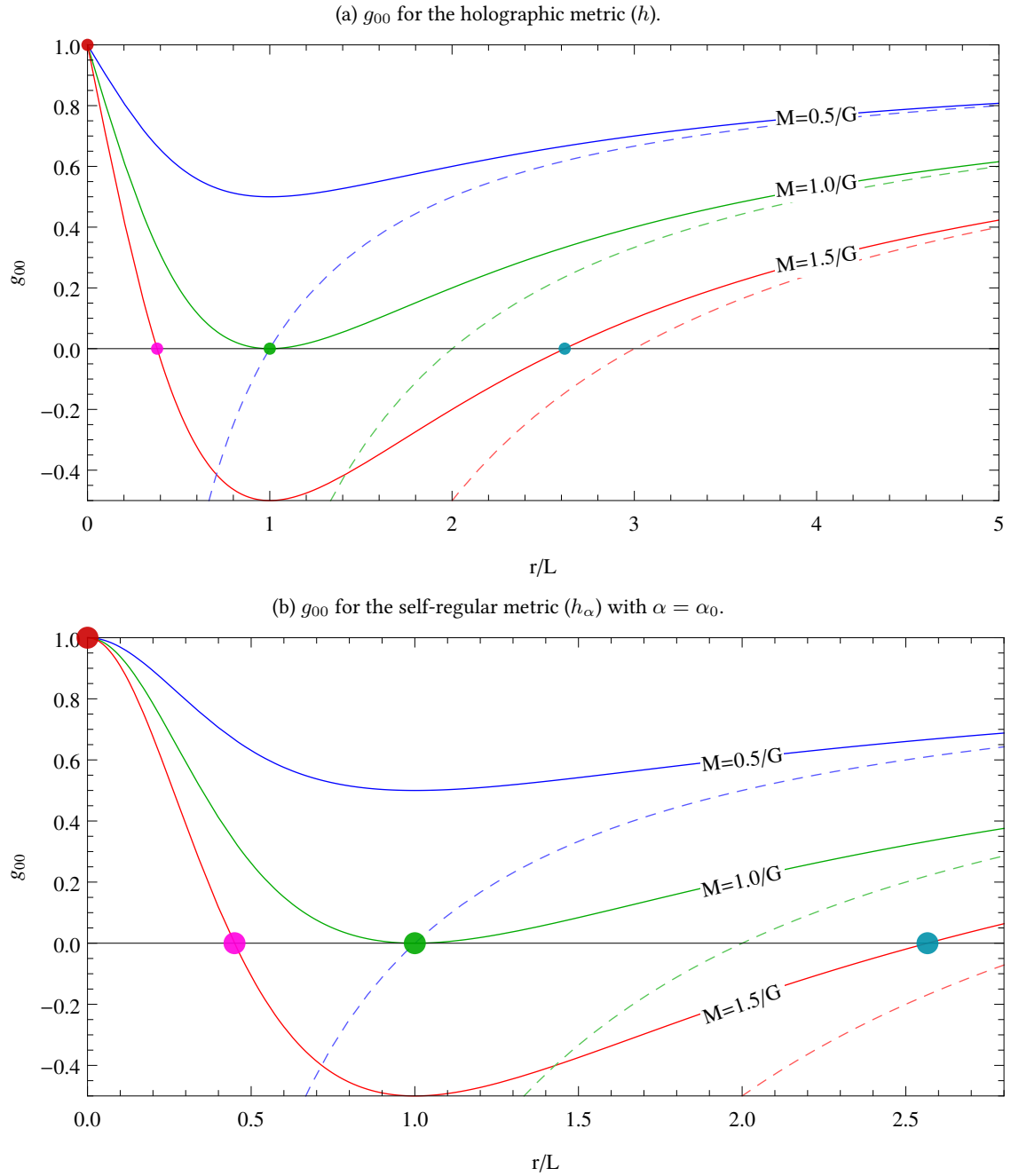(b) g_{00} for the self-regular metric (h_α) with $\alpha = \alpha_0$.

Figure 4.1: The big remnant picture for $n = 0$. The three curves represent a smaller than critical-mass (blue), critical mass (green) and a too heavy mass (red). In any case the dashed line corresponds to the equivalent Schwarzschild metric. Note the different behaviour as $z = r/L \to 0$.
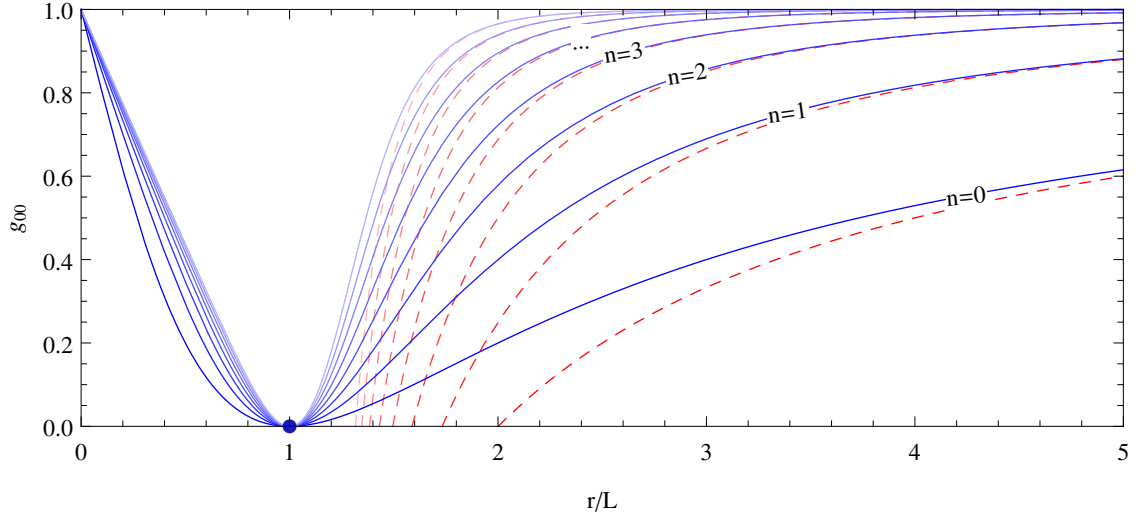
Figure 4.2: The holographic metric in the extra dimension scenario, compared with the Schwarzschild-Tangherlini metric (dashed line), for the self-encoding masses M_*. All curves are scaled for the individual L_* according to the numerical values given in table 4.1.

Compared to the fourdimensional metric (fig. 4.1a), we see that the picture basically *stays the same*. In this figure, the curves qualitatively get "sharper" with increasing n, which corresponds to the increasing surface to volume ratio of n-spheres, which is a purely geometrical effect.

4.2 Horizons

The event horizon equation, considering r_H being the event horizon, requires $0 = g_{00}(r_H)$. For my choices of $H(r)$, the horizons r_H are given by the roots of the polynomials

$$0 = z^{2+n} - z\, m_n + 1 \qquad \text{for } h(r) \tag{4.5a}$$

$$0 = z^2 (z^\alpha + {}^1\!/_2)^{(3+n)/\alpha} - m_n \quad \text{for } h_\alpha(r), \tag{4.5b}$$

with $m_n = 2/(n+2)M/M_*^{n+2}$ and $z = r/L$. The number of (physically meaningful) solutions depends on m_n, that is, on the Black Hole mass M. For any n, there are three possible solutions, plotted in figure 4.1:

$M < M_*$ The mass is to small to create a black hole. In the case of the self-regular metric, thy physical object is called a *G-lump* after Dymnikova [21] and represents a vacuum, self-gravitating, regular, particle-like structure [1].

$M > M_*$ There a two horizons with radii $r_\pm$. In figure 4.1, they are indicated by red dots. Physically, we will argue that the outer horizon r_+ is the more relevant one, since it *shields* the black hole inner structure. Mathematically, r_- is a cauchy horizon, and in the region $r_- < r < r_+$, where $g_{00} < 0$ and $g_{rr} > 0$, the coordinates r and t change their meaning.

There are no meaningful compact analytic expressions for the values of $r_\pm$, expcept for the holographic metric and without extra dimensions ($n = 0$), as given in already [53]:

$$r_\pm = GM \pm \sqrt{G^2 M^2 - 4}. \tag{4.6}$$

For $n > 0$ and especially for the self-regular metric, the roots of (4.5) can simply be determined numerically.

Note that for $M \gg M_*$, r_+ approaches the Schwarzschild-Tangherlini horizon.

	n	0	1	2	3	4	5	6	7
	L_*	1.00	0.79	0.76	0.76	0.76	0.77	0.78	0.79
h	M_*	1.00	1.26	1.32	1.32	1.31	1.29	1.28	1.26
	G_*	1.00	1.59	1.73	1.74	1.71	1.67	1.63	1.59
	α_0	1.755	4.285	7.081	9.333	10.642	11.128	11.098	10.805
h_α	L_*	1.	0.851	0.856	0.862	0.86	0.851	0.839	0.825
	M_*	1.	1.176	1.168	1.16	1.163	1.175	1.192	1.212
	G_*	1.	0.724	0.733	0.743	0.739	0.725	0.704	0.681

Table 4.1: Equations (4.9) in numbers: The self-encoding horizon radius $r_0 = L_*$, remnant masses $M_* = 1/L_*$ and reduced coupling (Newtons) constant $G_* = M_*^2$. These numbers are given in multiple of $L_P = \sqrt{\hbar G/c^3} \approx 10^{-35}$ m, the 4d Planck unit. For the self-encoding model, all values are given for $\alpha = \alpha_0$ (also displayed), as derived in equation (4.14).

$M = M_*$ The two horizons merge to a single horizon which we call $r_\pm = r_0$. This is the *extremal* radius, identified with the extremal mass M_*. In figure 4.1, the green line displays the gravitational potential with extremal mass, showing a single horizon, indicated by the green dot.

4.3 The Self-encoding remnant

The extremal black hole configuration $M = M_*$ is a feature of the nonlocal matter density. This configuration has special thermodynamical properties which we will discuss in the next chapter. First, we clear the situation of length scales of our models $H(r)$. We find the extremal radius r_0 with the remnant equations:

$$\begin{cases} \partial_r|_{r=r_0}\, g_{00}(r) & = 0 \\ g_{00}(r_0) & = 0 \end{cases} \tag{4.7}$$

For our generic potential (3.29), we rewrite the first equation to

$$\partial_r V(r) = 0 = -(n+1)\frac{H+(r)}{r} + H'(r) = L\,H'(z) - \frac{n+1}{z}\,H(z) \tag{4.8}$$

This equation can be solved for both $h(r_0)$ and $h_\alpha(r_{0,\alpha})$. We end up with

$$r_0 = \tilde{r}_0 \left(\frac{1}{1+n}\right)^{\frac{1}{2+n}} \quad \text{and} \quad r_{0,\alpha} = \tilde{r}_0 \left(\frac{1}{1+n}\right)^{\frac{1}{\alpha}}. \tag{4.9a, 4.9b}$$

Equation (4.9) enables us to connect the length scale $\tilde{r}_0$ introduced for the holographic and self-regular model to a physical length scale r_0. Note that the *self-encoding* principle requires that the size of the remnant r_0 should be identical to the fundamental length scale of the physical theory l_0. For gravity in 4d space time, the only fundamental length scale is given by the coupling constant (Newtons constant) G which defines the Planck length $L_{\text{Pl}} = \sqrt{G} \approx 10^{-35}$ m. In 4d, (4.9) assures this is true, as already stated in [53]:

$$r_0 \stackrel{!}{=} l_0 = L_{\text{Pl}} = \tilde{r}_0. \tag{4.10}$$

With extra dimensions, there is the reduced Planck length L_* which is the actual fundamental length scale l_0, since the observable Planck length L_{Pl} is just an effective one. To express $h(r)$ and $h_\alpha(r)$ only in terms of L_*, we require $r_0 \stackrel{!}{=} l_0 = L_*$ and find

$$\tilde{r}_0 = (1+n)^{\frac{1}{2+n}}\, L_* \quad \text{and accordingly} \quad \tilde{r}_0 = (1+n)^{\frac{1}{\alpha}}\, L_*. \tag{4.11a, 4.11b}$$

When computing $M(r_0)$, we also expect the self-encoding of the fundamental mass scale M_*, that is, $M(r_0) = M_*$. For the holographic metric, it is $h(L_*) = 1/(2+n)$ and thus

$$M(L_*) = \frac{2}{n+2} \left(\frac{L_*}{L_*}\right)^{1+n} \frac{1}{h(L_*)} M_* = \boxed{2} \, M_*. \tag{4.12}$$

In case of the self-regular metric, α must be fixed to ensure $M(r_0) = M_*$. Using the mass (4.4), it reads (2 weggemogelt)

$$M(r_H) = \underbrace{\frac{1}{n+2} \left(\frac{3+n}{2}\right)^{\frac{3+n}{\alpha}}}_{\overset{!}{=}1} \left(\frac{r_0}{L_*}\right)^{n+1} M_* = M_* \quad \text{with } \alpha = \alpha_0 \tag{4.13}$$

This gives us the self-encoding value for the α parameter:

$$\alpha_0 = \frac{3+n}{\ln(2+n)} \ln \frac{3+n}{2}. \tag{4.14}$$

4.4   The regular core

As announced in section 3.6, the self-regular metric offers a non-diverging curvature at the origin. The Ricci scalar is given by, according to (3.21),

$$R(r) = R_N^N = \frac{(n+2)V(r)}{r^2} + V''(r) \tag{4.15a}$$

$$= \frac{2}{2+n} \frac{M}{M_*^{2+n}} \frac{(2+n)^2 H(r) - 2(1+n)rH'(r) + r^2 H''(r)}{r^{3+n}} \tag{4.15b}$$

We can give an estimation for $R(0)$ based on the taylor expansions of $H(r)$ at $r = 0$:

$$h(r) = (r/L)^{2+n} + \mathcal{O}\left((r/L)^{2(2+n)}\right), h'(r) \approx (r/L)^{1+n}, h''(r) \approx (r/L)^n \tag{4.16}$$

$$h_\alpha(r) = (r/L)^{3+n} + \mathcal{O}\left((r/L)^{2(3+n)}\right), h_\alpha'(r) \approx (r/L)^{2+n}, h_\alpha''(r) \approx (r/L)^{1+n} \tag{4.17}$$

Inserting this into $R(r)$ for $H(r)$, equation (4.15b), gives $H(0) \approx L/r$ for the holographic metric whereas the self-regular metric exposes a finite value at $R(0)$ as soon as $\alpha > 0$, c.f. figure 4.3. This is the reason for the naming of the self-regular metric.

Actually there are reviews about the quite general family of regular black holes, e.g. by Ansoldi [1] or Hayward [31]. As we see in the next section 4.5 about their conformal picture, regular Black holes enjoy special properties.

4.4.1   The limit $\alpha \to \infty$

To learn more about the origin of the regularity, let's investigate the limit $\alpha \to \infty$, plotted in figure 4.4. At $\alpha \to \infty$, the two phases of the black hole clearly stand out. Let's discuss the case for simplicity in $n = 0$ and $M = M_*$. It is

$$\lim_{\alpha \to \infty} g_{00} = \begin{cases} 1 - 2GMr^2 & , r < L \\ 1 - \frac{2GM}{r} & , r > L. \end{cases} \tag{4.18}$$

We recognize the deSitter space gravitational potential from section 2.2.3,

$$g_{00} = 1 - \frac{\Lambda}{3} r^2, \tag{2.20 revisited}$$

with positive cosmological constant $\Lambda = {}^2\!/\!{}_3 \, GM$ and positive constant curvature $R = 4$ (c.f. figure 4.3). This is called the deSitter *core* since for physical meaningful theories, $r < \infty$.
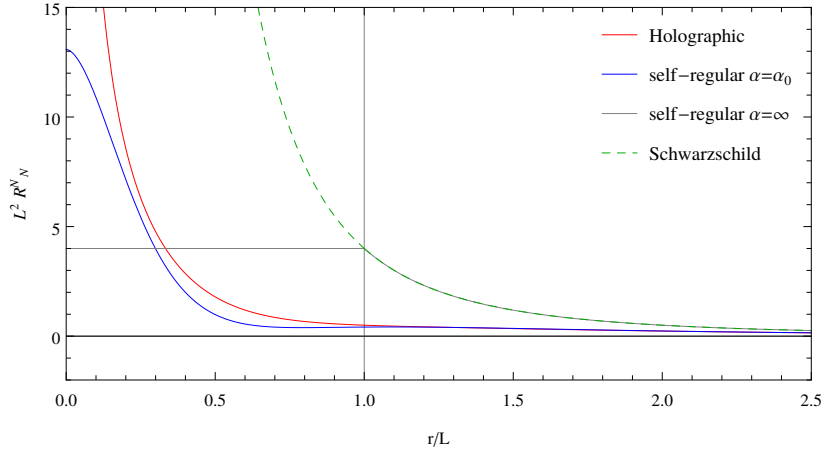
Figure 4.3: The curvature scalar R for $n = 0$, $GM = 1$, $\alpha = 3\alpha_0$ holographic (red) and self-regular model (blue). While the curvature diverges for the holographic black hole, any value of the self-regular black hole archives a finite value $R(0)$.

What's the meaning of the cosmological vacuum solution like deSitter in the context of quantum black holes? EFE relate space time $G_{\mu\nu}$ to matter density $T_{\mu\nu}$. In this thesis we will frequently encounter the term *dual theory* which means shifting contributions between $G_{\mu\nu}$ and $T_{\mu\nu}$. In this mind, the dual theory to deSitter space-time as a solution of EFEs with cosmological constant and zero energy momentum tensor $T_{\mu\nu}$ is EFE without cosmological constant but shifted contributions inside the energy momentum tensor. This idea goes back to Dymnikova [21]. In the quantum picture, this is interpreted as the *Quantum Vacuum* and is characterized by it's *outward pressure* we were encountered with already at the time of the derivation of the black hole, equation (3.19) that defines the tangential pressure as

$$p = \rho + \frac{r}{n+2} \partial_r \rho > 0. \tag{4.19}$$

We can imagine this type of pressure as the fermi gas and refer to the pressure as degeneracy pressure. This kind of pressure also prevents the G-lump from collapsing in it's own gravitational inwards pressure.

For a review about regular interiors of Schwarzschild-like black holes with $T_0^0 = T_1^1$, see also [22].
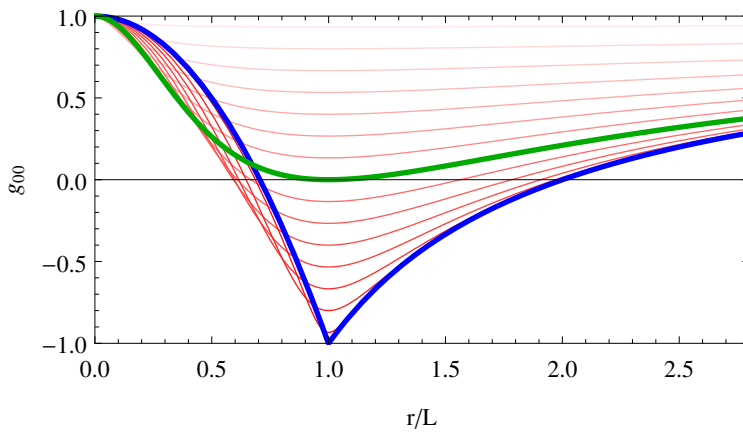

Figure 4.4: Self-regular: g_{00} for $M = 1$ and different choices of $\alpha \in \{0, 20\}$. The blue curve shows the limit $\alpha \to \infty$ where the behaviour is clearly separated: For $r < L$ there is a Desitter metric, above $r > L$ there is a Schwarzschild metric. Color saturation encodes the α scale. The special self-encoding choice $\alpha = \alpha_0$ is highlighted as green line, corresponding to figure 4.1b.
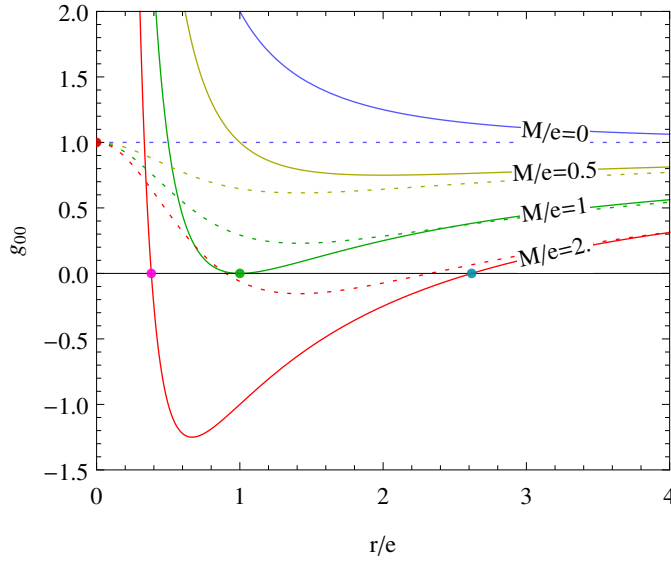
Figure 4.5: The Reissner-Nordström gravitational potential for different mass-charge ratios M/e, compared with the Bardeen solution for the same mass-charge ratios (dashed lines).

4.5 Conformal Structure

It is often helpful to transform coordinates in a way that the global structure of space-time is mapped on a finite diagram. If this mapping is conformal (preserving angles locally) and two-dimensional, such diagrams are called *(Carter-)Penrose diagrams* (after the british physican Roger Penrose). Penrose diagrams subject to any GR textbook that deals with black holes (e.g [30, 43, 71]) and I refer there for futher details.

The three Penrose diagrams that represent the three possible spacetimes presented in section 4.2 are displayed in figure 4.6. It is the diagram of a *regular black hole* which is resembles the structure of the *Reissner Nordström* (RN) black hole which describes static nonrotating black holes with electrical charge e in $d = 4$ (with $G = 4\pi\epsilon_0 = c = 1$),

$$V(r) = \frac{2M}{r} - \frac{e^2}{r^2} = 2\frac{M}{e}\frac{z-1}{z^2} \quad \text{with } z = r/e, \tag{4.20}$$

but singularity-free in the case of the regular black hole. This similarity dates back to the regular black hole by Bardeen (reviewd e.g in [1]), given by the gravitational potential

$$V(r) = \frac{2Mr^2}{(r^2 + e^2)^{3/2}} = 2\frac{M}{e}\frac{1}{(1 + e^2/r^2)^{3/2}}. \tag{4.21}$$

The Bardeen metric a special case of the self-regular black hole with parameters $\alpha = 2$, $\tilde{r}_0 = 2^{1/\alpha}e$ and is shown against the RN black hole in figure [?]. In this figure, one sees that the hyper-extreme case $M < e$ is replaced by G-lumps, giving flat space for $M/e \to 0$. This cures both the naked singularity as well as the repulsive gravity regime ($g_{00} > 1$).

Let's discuss the penrose diagrams shortly without going into detail how to find the maximally extended space-time that describes space-time everywhere, taking up the distinction of cases in section 4.2. Figure 4.6 contains three panels:

(a) The G-lump is probably the biggest archievement for the charged black hole, as it cures the naked singularity, while it is not the object of interest in our context.

(b) The conformal diagram for the maximally extended black hole is periodic on the vertical axis on infinite extend ("isometric" regions). There are three classes of regions: the untrapped and asymptotically flat space time region **I**. The timelike region of trapped surfaces **II**, characterized by $r_- < r < r_+$, connects outer **I** and core **III** regions. The again spacelike and untrapped region **III** is hyperbolic, as dominated by deSitter behaviour. Note that in this space-time, it is possible to *wrap*
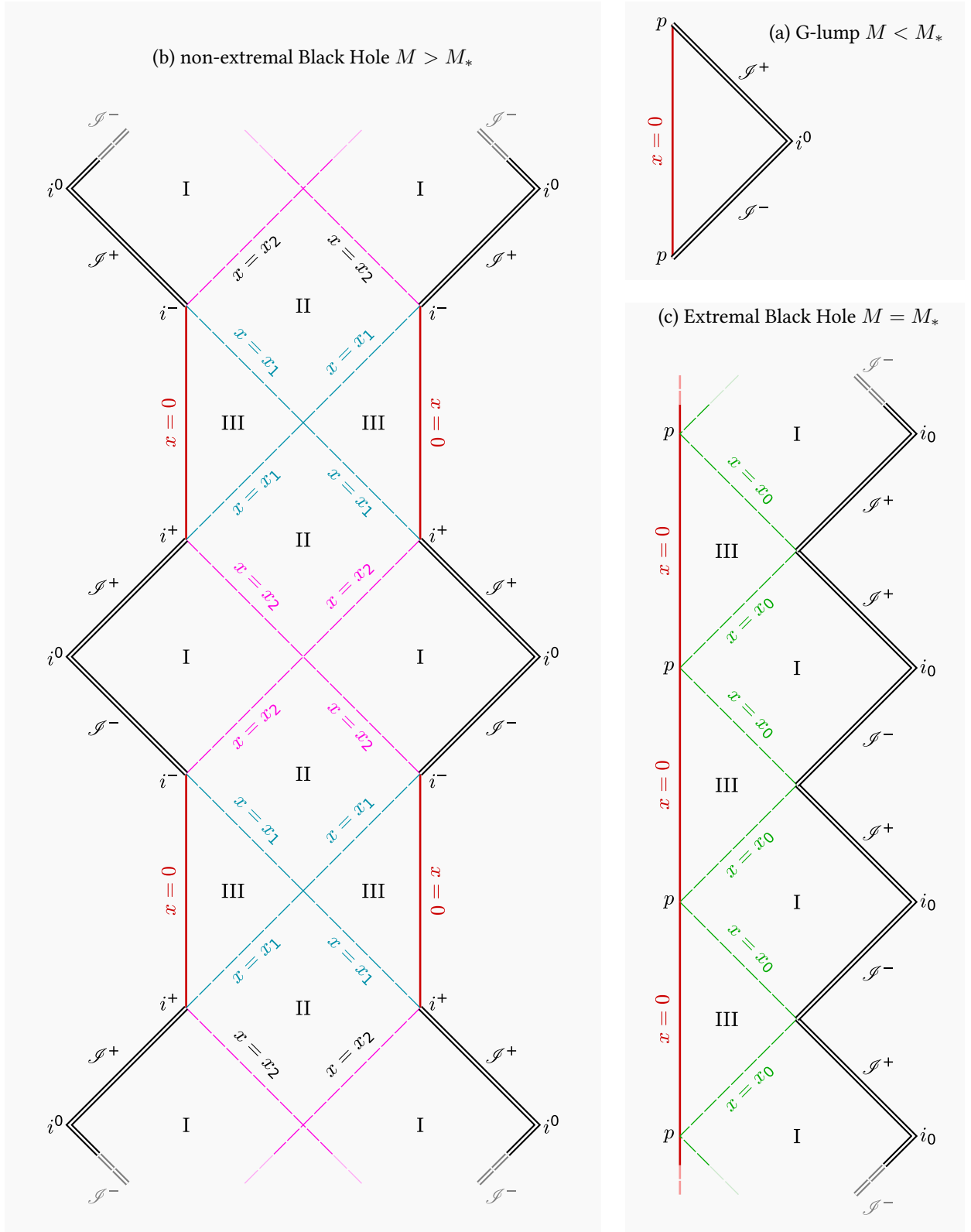
Figure 4.6: The penrose diagrams of the regular black holes, after [1,31,46]. x is a dimensionless coordinate $x = r/e$ and $x_2 = r_+/e$ is the outer horizon, while $x_1 = r_-/e$ is the inner horizon. $x_0 = r_0/e$ is the extremal horizon. The colors of constant horizons x in these diagrams match the colors of the according coordinates in figure 4.1 and 4.5. This diagram is basically the same for both Reissner Nordström and the holographic metric, where there are singularities at $x = 0$.

around the universe by starting from **I**, travelling **II** and **III** and leaving the black hole near-zone again over **II** to **I**, all inside a causal light-cone with $45°$ angles.

(c) The extremal situation also made the singularity accessible from outside by travelling from region **I** to **III**. This is cured with a regular origin.

4.6   Energy conditions

Energy conditions in general relativity are a tool to put constraints on matter distributions (that is, energy-momentum tensors) in a way how some expects them to behave. They are formulated from a classical viewpoint and not deduced from Einstein field equations or other first principles. Roughly speaking, they generalize the statement that one does not observe negative masses or regions of negative mass distribution.

Approaches to quantum gravity regularly violate energy conditions, and by examining how and where they violate these conditions, one understands about the quantum nature in general relativity. For example, one expects energy conditions in delta smearing densities to be local around the black hole, e.g. violations occur in a region $r \lesssim L_*$ while they hold for $r \gtrsim L_*$. As Ansoldi notes, this is cannot be taken for granted in a non linear theory as general relativity is [1].

Perhaps nice to remember:

- Trace EC: Density must at least equal the sum of the principal pressures

- Strong EC: Matter must gravitate toward matter

- Dominant EC: Energy must not flow faster than light

- Weak EC: Local mass-energy density must not be negative

- Null EC: Stress-energy experienced by a light ray must not be negative

Pending: Plot energy conditions of my BHs (siehe BN2010).

Chapter 5

Thermodynamical properties

This chapter is dedicated the derivation and discussion of the temperature, stability and entropy of the black hole remnant. This means the non-extremal black hole configurations are no more discussed here.

Law	Thermodynamics	Black Holes
0.	T constant on a body in thermal equilibrium	κ constant on horizon of (stationary) BH
1.	$\mathrm{d}E = T\mathrm{d}S - p\mathrm{d}V + \mu\mathrm{d}N$	$\mathrm{d}M = \frac{\kappa}{8\pi}\mathrm{d}A + \Omega_H\mathrm{d}J + \Phi\mathrm{d}q$
2.	$\delta S \geq 0$	$\delta A \geq 0$
3.	$T = 0$ cannot be reached	$\kappa = 0$ cannot be reached

Table 5.1: The laws of thermodynamics correspond with Black hole thermodynamics

5.1   Hawking Temperature

The Hawking temperature $T_H = \kappa/4\pi$ is defined by means of the surface gravity $\kappa = \partial_r g_{00}|_{r=r_H}$. Here, we insert $r_H = r_0$ and get for generic $H(r)$ the temperature

$$T_H = \frac{1}{4\pi}\left(\frac{1+n}{r_H} - \frac{H'(r_H)}{H(r_H)}\right).$$
(5.1)

Taking the Schwarzschild limit according to section 3.6.3, we let $H'/H \to 0$ and evventually get the well known 4d Schwarzschild temperature $T = 1/(4\pi r_H)$. The H'/H term is the quantum correction.

It is simple to insert our $\{h, h_\alpha\} \in H$. Figure 5.1 shows T_H for both of them. For the sake of completeness, we give T_H for both models here explicit:

$$T_H = \frac{1}{4\pi r_H}\left(1 + n - (2+n)\frac{(L/r)^{(2+n)}}{1 + (L/r)^{(2+n)}}\right) \quad \text{for } h(r)$$
(5.2)

$$T_H = \frac{1}{4\pi r_H}\left(1 + n - \frac{(L/r)^{4+n}}{1 + \frac{1}{\alpha}(L/r)^{3+n}}\right) \quad \text{for } h_\alpha(r)$$
(5.3)

Below $r \lesssim 3L_p$, the Hawking temperature differs significantly from the Hawking temperature. There is a maximum temperature at a critical radius r_C (indicated by the dots in fig. 5.1, numerical values are given in table 5.2), and for smaller radius the black hole cools down until it reaches zero temperature at $r_H = r_C$. We therefore speak of an *cold* remnant.

This result significantly stands in contradiction to the laws of thermodynamics, a zero temperature object shall not exist. I currently don't know how this is treated.
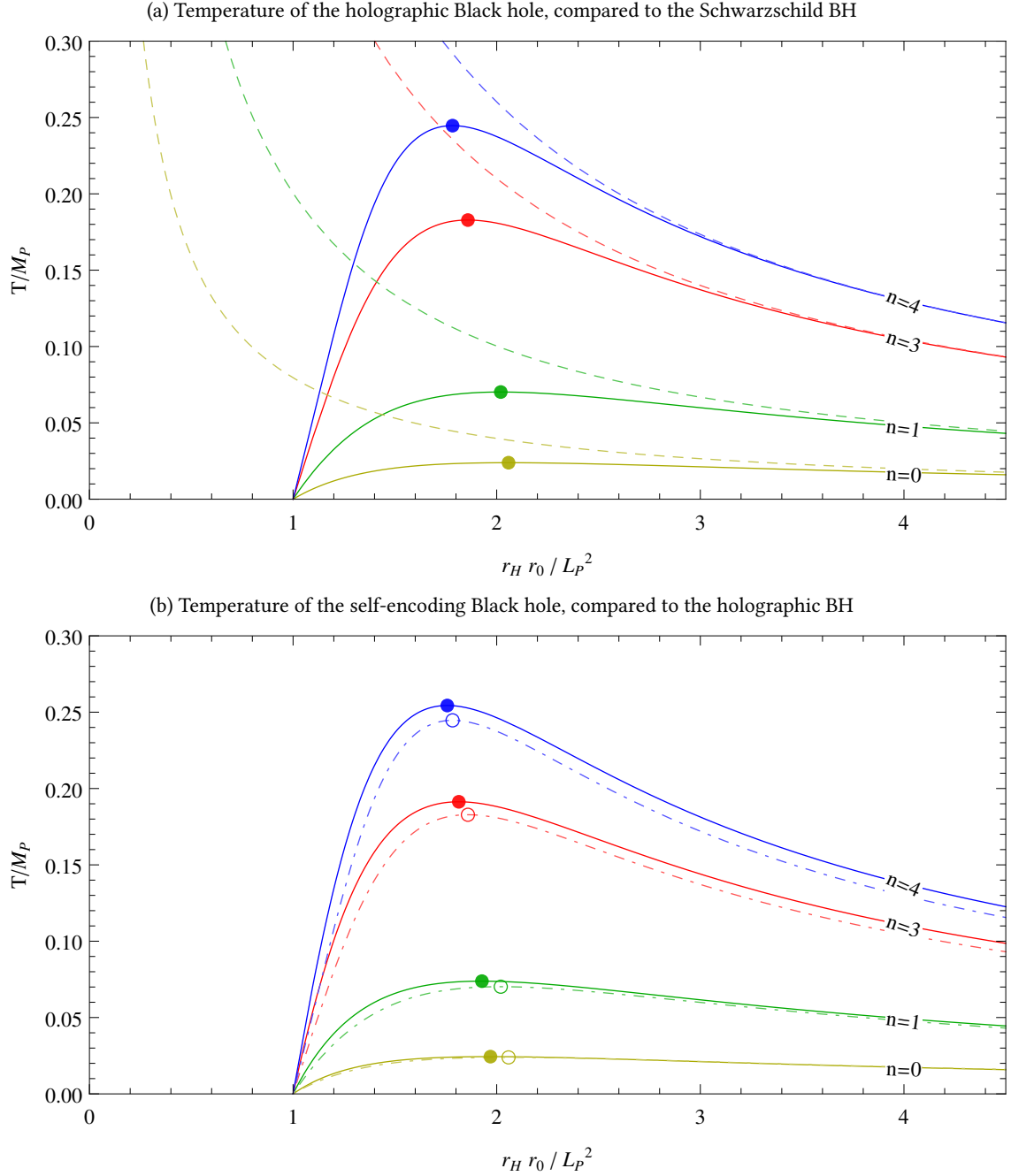
(a) Temperature of the holographic Black hole, compared to the Schwarzschild BH

(b) Temperature of the self-encoding Black hole, compared to the holographic BH

Figure 5.1: Temperature of the Black Holes for different extra dimensions n. While the x-axis scaling depends on n (r_0 given in equation 4.9a), the y-axis is scaled by ordinary L_P (Das ist Quatsch! $[T] = M$!) in 4 dimensions, to show the increasing heat. The circles indicate the critical radii.

In frame (a), the dashed lines corresponds to the classical Hawking-Beckenstein temperature of the Schwarzschild-Tangherlini metric in n extra dimensions. In frame (b), the dot-dashed line indicates the corresponding temperatures of the holographic metric.

n	0	1	2	3	4	5	6	7
r_C	2.060	1.600	1.480	1.410	1.360	1.330	1.300	1.280
r_{C,α_0}	1.970	1.460	1.340	1.290	1.260	1.250	1.230	1.220
$T(r_C)$	0.024	0.070	0.124	0.183	0.245	0.309	0.375	0.443
$T(r_{C,\alpha_0})$	0.024	0.074	0.131	0.191	0.254	0.319	0.386	0.454

Table 5.2: Critical radii r_C for different dimensions, for the holographic (r_C) and self-regular (r_{C,α_0}, so $\alpha = \alpha_0$) black holes, and maximum temperatures of the according black holes. All values are given in 4d Planck units.

5.2   Heat Capacity

The heat capacity is an extensiv thermodynamical property, defined as measure of the heat added to an object resulting from a temperature change, in terms

$$C = \frac{Q}{\Delta T}. \tag{5.4}$$

For Black Hole thermodynamics, we identify $Q = M$ and use the Hawking temperature just derived to compute the heat capacity. Since it is virtually not possible to exress $M = M(T_H)$, we insert $1 = \partial r_H / \partial r_H$ and compute

$$C = \frac{\partial M}{\partial T_H} = \frac{\partial M}{\partial r_H} \left(\frac{\partial T_H}{\partial r_H} \right)^{-1} = \frac{\partial M}{\partial z_H} \left(\frac{\partial T_H}{\partial z_H} \right)^{-1}. \tag{5.5}$$

For generic $H(r)$, inserting temperature (5.1) and mass (4.4), one can do the elaborate computation and ends with the compact expression

$$C = \frac{4\pi r_H^{n+2}}{A\bigstar\heartsuit} \frac{r_H H'(r_H) - (n+1)H(r_H)}{r_H^2 H(r_H)H''(r_H) - r_H^2 H'(r_H)^2 + (n+1)H(r_H)^2} \tag{5.6}$$

Now inserting choices for $H(r)$ is quickly done. Figure 5.2 shows the graph of C for the holographic and self-encoding metric.

By simply letting $H, H', H'' \to 0$ according to section 3.6.3, we end up with the diverging heat capacity of ordinary Schwarzschild black hole:

$$C \xrightarrow{H \to \delta} -2(2+n)\pi M_*^{2+n}\Omega_{2+n} r_H^{2+n} \xrightarrow{n \to 0} -\frac{4\pi r_H^{2+n}}{2G} \tag{5.7}$$

And now the same as commutation diagram (testing):

$$
\begin{array}{ccc}
C & \xrightarrow{\quad H \to \delta \quad} & -2(2+n)\pi M_*^{2+n} r_H^{2+n} \\
{\scriptstyle n \to 0}\Big\downarrow & & \Big\downarrow{\scriptstyle n \to 0} \\
\frac{4\pi r_H^2}{A} \frac{r_H H' - H}{r_H^2 H H'' - r_H^2 H'^2 + H^2} & \xrightarrow{\quad H \to \delta \quad} & -\frac{4\pi r_H^{2+n}}{2G}
\end{array}
\tag{5.8}
$$

In contrast to the Schwarzschild solution, for our choice of smeared $H(r)$, the heat capacity undertakes two changes of sign, one of them when a phase transition takes place ($C \to \pm\infty$). We call this critical radius r_C. At this point, the Black Hole temperature $T_H(r_C)$ (eq. 5.1) is maximal:

$$\partial_{r_H} T_H |_{r_H = r_C} = 0 \Leftrightarrow z_C = \sqrt{\frac{1+n}{H'(z_C) - H''(z_C)H(z_C)}} H(z_C). \tag{5.9}$$

(a) Heat Capacity of the holographic Black hole, compared to the Schwarzschild BH

(b) Heat Capacity of the self-encoding Black hole, compared to the holographic BH
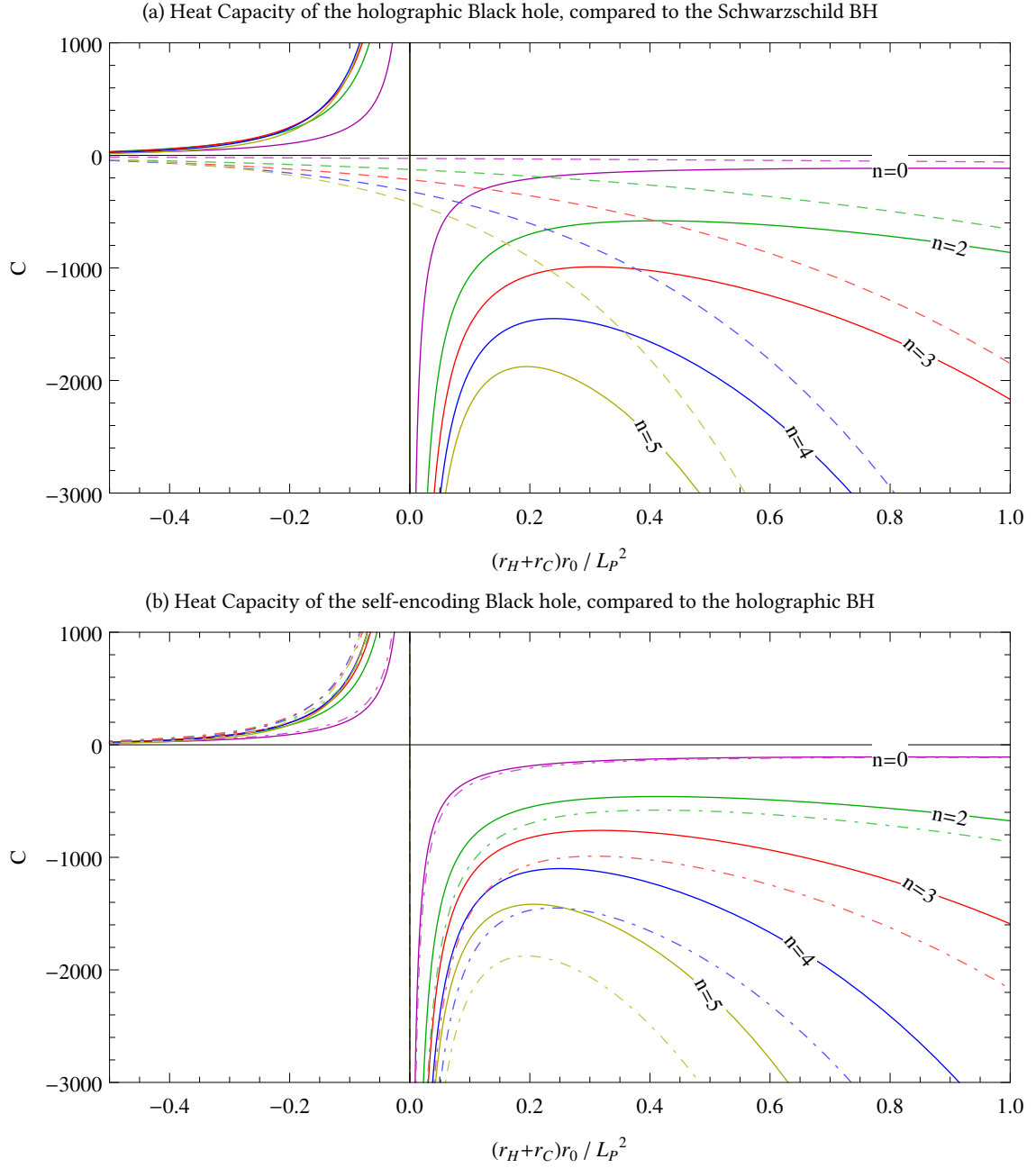
Figure 5.2: Heat Capacity of Black Holes for different extra dimensions n. For each dimensions n, the x-axis is shifted to the critical radius and scaled by the horizon length r_0 as given in equation 4.9a.
In frame (a), the dashed lines corresponds to the heat capacity of the classical Hawking-Beckenstein black hole in n extra dimensions. In frame (b), the dot-dashed line corresponds to the corresponding heat capacity of the holographic metric.

The expression (5.9) suggests investigating the $H(z) \to \Theta(z)$ limit, but of course the Schwarzschild black hole has no extremal temperature. Mathematically, $z_C \to \infty$, but there is no physical content in this result.

The critical radius for $h(r_C)$ and $h_\alpha(r_{C,\alpha})$ can be determined by evaluating the extremal temperature condition (5.9):

$$r_C = 2^{\frac{1}{n+2}} \left((2+n)\sqrt{n^2 + 2n + 5} - n^2 + 3n - 4 \right)^{-\frac{1}{n+2}} L, \tag{5.10}$$

$$r_{C,\alpha} = 2^{\frac{1}{\alpha}} \left(\sqrt{(3+n)(3+n+\alpha(2+3\alpha+(\alpha-2)n))} + (n-1) - \alpha(3+n) \right)^{-\frac{1}{\alpha}} L. \tag{5.11}$$

The critical radius was used to rescale the abscissa in figure 5.2, so $(r_H - r_C)r_0$ is displayed. Thus it is easier to compare C for a different number of dimensions. Numerical values for r_C are given in table 5.2.

5.3 The Phase transition

Evventually, now having computed g_{00}, T and C enables us comparing those for Black Hole stability discussion. Figure 5.3 illustrates the curves and different phases of the holographic black hole. Considering the sign of the heat capacity, we distinguish three phases:

$r > r_c$. The Heat Capacity is negative, the system is instable: Loosing mass by radiation makes it hotter and hotter. This behaviour is well described by the Schwarzschild metric.

When reaching $r \to^+ r_c$, in our modified metrics this process stagnates, the temperature no more rises. Now a phase transition takes place at r_C, the system suddenly get's stable.

$r_0 < r < r_C$. The Heat Capacity is positive and the black hole system is stable. Loosing mass now results in loosing temperature. The system heavily deviates from the classical Schwarzschild solution. The Temperature decreases until it evventually reaches zero.

$r < r_0$. There is an event horizon at r_0 which is possibly the smalles possible event horizon, rejecting the answers for questions after physical properties beyond the reason. In this model, the Heat Capacity again get's negative, but in the same way the temperature get's negative, giving rise to it's physical interpretation.
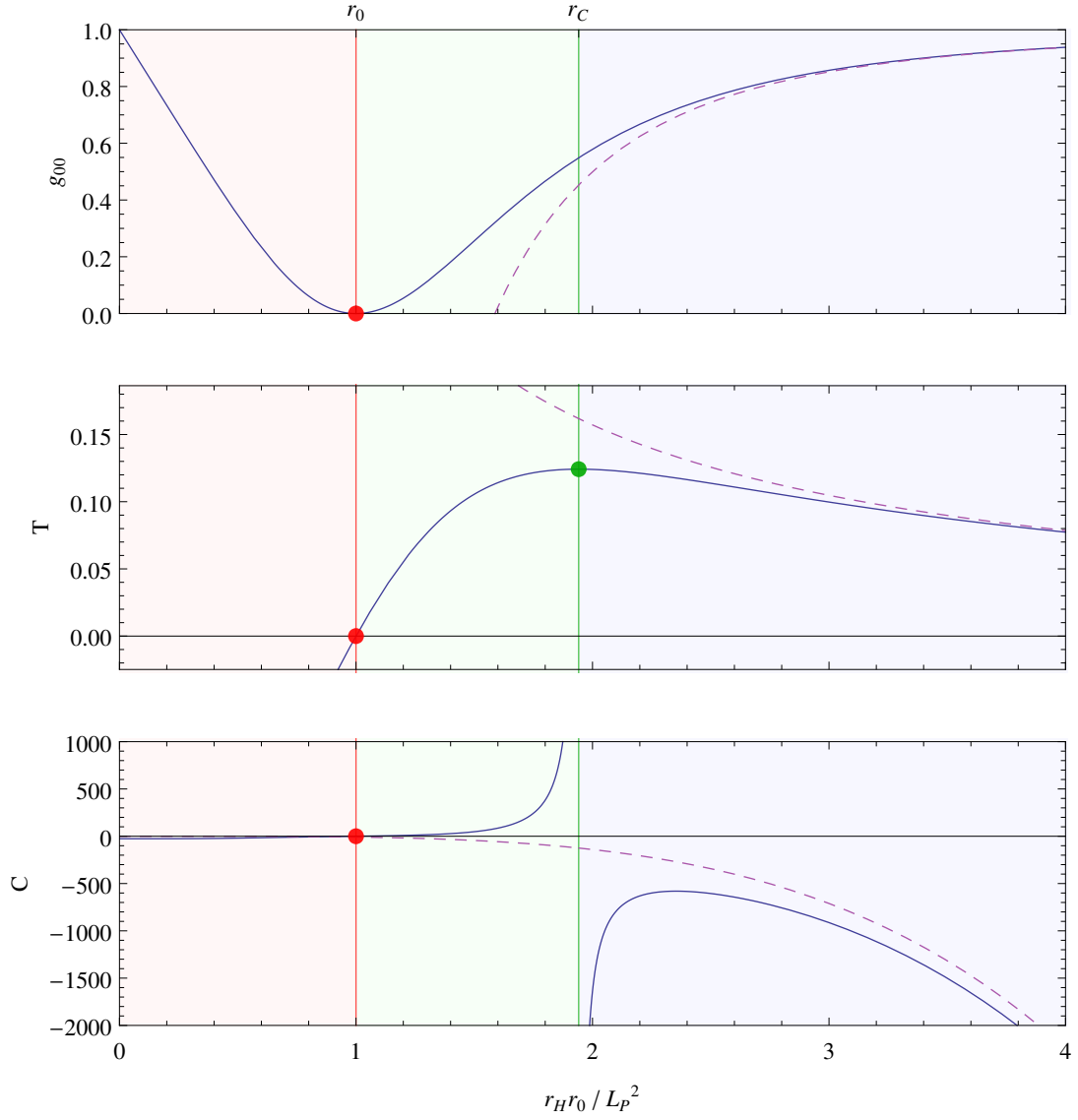
Figure 5.3: Comparison of first metric coefficient (g_{00}, top panel), temperature (middle panel) and heat capacity (bottom panel) on the same scale. The blue curve represents the holographic black hole for an arbitrary dimension (here: $n = 2$). The dashed curve is the corresponding Schwarzschild behaviour. Regarding the sign of the heat capacity (Sign $C = \pm 1$), there are three different states, indicated by colors and seperated by r_0 (red line) and r_C (green line).
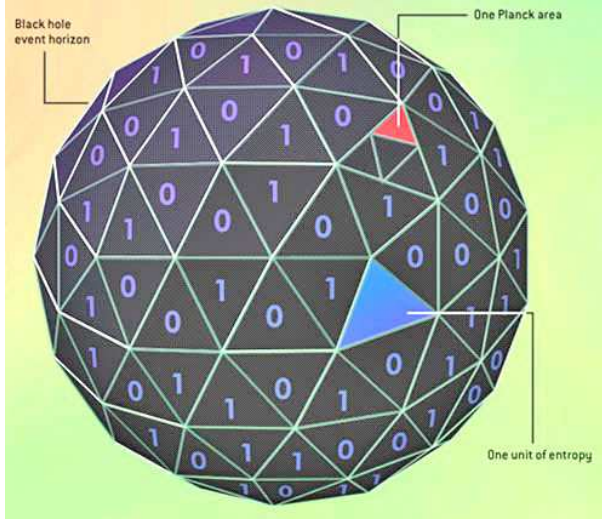
Figure 5.4: An artistic interpretation of the holographic principle, as it illustrated an science magazine article by Jacob Bekenstein [7]. The Black Hole entropy is quantizied in terms of planck units. A planck area (blue) has $A/4$ units of entropy (red).

5.4 Entropy

Entropy as a measure for micro states in a thermodynamical system is in the context of Black holes thermodynamics maybe the most interesting quantity. We define entropy as

$$S = \int \frac{\mathrm{d}M}{T} \tag{5.12}$$

The entropy defining integral can also be subsituted like in the Heat Capacity in the section before, giving for generic H a compact expression:

$$S(r) = \int \frac{\mathrm{d}M}{T} = \int \mathrm{d}r_H \left(\frac{1}{T} \frac{\mathrm{d}M}{\mathrm{d}r_H} \right) = 4\pi m_n \int \mathrm{d}r_H \frac{r_H^{1+n}}{H(r_H)} \tag{5.13}$$

Making the limit $H \to \Theta$, we immediately get the Schwarzschild entropy curve

$$4\pi m_n \int \mathrm{d}r_H \ r_H^{1+n} = \frac{4\pi m_n}{1+n} r_H^{2+n} \xrightarrow{n \to 0} 8\pi G \ r_H^2 \tag{5.14}$$

Compared to that curve, for the holographic model in n dimensions the entropy integral (5.13) has the value

$$S_h(r) = 4\pi m_n \left(\frac{r^{n+2}}{n+2} + \log(r) \right). \tag{5.15}$$

Notice the *logarithmic quantum corrections*. At the end of the day, they motivate the label *holographic* for the $h(r)$-smeared metric. If I would not have modified the metric for higher dimensions, the entropy (for $h(r) = 1/(1 + (L/r)^2)$ in any n) would look as

$$S = 4\pi m_n \left(\frac{r^{n+2}}{n+2} + \frac{r^n}{n} \right) \quad \text{for } n > 0. \tag{5.16}$$

The self-encoding metric also does not possess a logarithmic entropy correction, but a hypergeometrical one:

$$S = \frac{4\pi m_n}{n+2} \left(r^2 + {}_2F_1 \left(-\frac{2+n}{\alpha}, -\frac{3+n}{\alpha}, 1 - \frac{2+n}{\alpha}; -\frac{1}{2r^\alpha} \right) \right) \tag{5.17}$$

5.4.1 The Area quantization picture

The black hole area theorem dates back to Wheeler 1973 and is a recasting of the Schwarzschild black hole entropy in terms of the horizon area $A = 4\pi r_H^2$, and therewith $S = A/(4L_P^2)$.

This holds also for higher dimensions, where the surface is $A = \Omega_{n+2} r_H^{2+n}$ and we can recast the holographic metric black hole (5.15) as

$$S_h(A_+) = \frac{\pi}{A_0}(A_+ - A_0) + \pi \log(A_+/A_0). \tag{5.18}$$

Weiter: Oberflächenterme identifizieren (nicht $\mathcal{A}$), über Verschwinden von S, usw.

Casting entropy surface quantization etc...

Self-Completness of Einstein gravity [20] [19]

Chapter 6

Modified Field Equations

Modifying the Einstein equations means finding new field equations and therefore a more fundamental theory than before. This new theory has intrinsically built in support for nonlocality, that is, inserting the Schwarzschild density $\rho_\delta(r)$ gives the results discussed before. There is no more "need" for $\rho(r) \, H'(r)$ anymore.

The field equation modification can be introduced with a bilocal distribution $\mathcal{A}^2(x-y)$ in the Ricci Scalar R integral identity

$$R(x) = \int \mathrm{d}y \, \delta(x-y) R(x) \tag{6.1}$$

Replacing the Dirac delta by it's smeared version $\delta(x-y) \to \mathcal{A}^2(x-y)\delta(x-y)$ produces the smeared Ricci scalar (Wichtig: Wie genau ist die Definition von $\mathcal{A}$? Als Ersatz für δ oder drangepatscht?)

$$\mathcal{R}(x) = \int \mathrm{d}y \, \mathcal{A}^2(x-y) R(x). \tag{6.2}$$

It finally gives rise to the smeared energy-momentum tensor

$$\mathcal{T}_0^0 = -M\mathcal{A}^{-2}(\Box)\delta(\vec{x}). \tag{6.3}$$

We can identify that formalism with the formalism made before,

$$T_0^0 = -\frac{M}{\Omega_{n+2} \, r^{n+2}} \frac{\mathrm{d}H(r)}{\mathrm{d}r} \tag{6.4}$$

Matching equations (6.3) and (6.4) means

$$\mathcal{A}^{-2}(\Box)\delta(\vec{x}) = \frac{1}{\Omega_{n+2}r^{n+2}} \frac{\mathrm{d}H(x)}{\mathrm{d}x} \tag{6.5a}$$

Writing the dirac delta by it's plane wave momentum space representation $\delta(\vec{x}) = \int \mathrm{d}^{3+n}p \, e^{+ipx}$ on the left hand side and inserting a $1 = \mathcal{F}^{-1}\mathcal{F}$ by means of a double fourier transformation on the right hand side allows computing a solution for the operator in momentum space by means of a fourier transformation of the right hand side:

$$\Leftrightarrow \int \mathrm{d}p^{3+n} \, \mathcal{A}^{-2}(\Box) \, e^{ipx} = \frac{1}{\Omega_{n+2}r^{n+2}} \frac{\mathrm{d}H(x)}{\mathrm{d}x} \tag{6.5b}$$

$$\Leftrightarrow \int \mathrm{d}^{3+n}p \, \mathcal{A}^{-2}(p^2) \, e^{ipx} = \int \mathrm{d}^{3+n}p \, \overbrace{\left(\frac{1}{(2\pi)^{2+n}} \int \mathrm{d}^{3+n}z \frac{1}{\Omega_{n+2}\|z\|^{n+2}} \frac{\mathrm{d}H(\|z\|)}{\mathrm{d}\|z\|} e^{-ipz} \right)}^{\tilde{T}_0^0(p)} e^{ipx} \tag{6.5c}$$

$$\Leftrightarrow \mathcal{A}^{-2}(p^2) = \frac{1}{(2\pi)^{2+n}\Omega_{n+2}} \int \mathrm{d}^{3+n}z \frac{1}{z^{n+2}} \frac{\mathrm{d}H(z)}{\mathrm{d}z} e^{-ipz} \tag{6.5d}$$

Note that, by concept, the operator $\mathcal{A}^{-2}$ is dimensionless. We therefore can switch the coordinate system $(r, p) \to (z, q)$ without new prefactors.

6.1 Higher-dimensional Fourier Transformation

To solve (6.5d), I make sure of integrating out all extra dimensional angles and effectively reducing the higher-dimensional fourier transformation of the radial symmetric function to a one dimensional. Calling something like $V(r) := \frac{H'(r)}{r^{n+2}}$ the higher dimensional Fourier kernel, we will derive an effective one-dimensional fourier transformation in this section. This is motivated by the well-known three dimensional procedure which is more likely easier to read and given in appendix 6.2.2.

We start with the $N = n + 3$-dimensional fourier transformation and rewrite it into conventional polar coordinates.

$$\hat{V}(p) = \frac{1}{(2\pi)^{3+n}} \int d^{3+n}r \; e^{-i\vec{r}\cdot\vec{p}} V(r) \tag{6.6a}$$

$$= \frac{1}{(2\pi)^{3+n}} \int_0^\infty dr \; r^{2+n} \int_0^{2\pi} d\varphi \prod_{i=1}^{n+1} \int_0^\pi d\theta_i \sin^i(\theta_i) \; e^{-i\vec{r}\cdot\vec{p}} V(r) \tag{6.6b}$$

Now we use the angle θ_1 for identification with the inner scalar product angle $\vec{r}\cdot\vec{p} := rp\cos\theta_0$. We subsitute $\int_0^\pi d\theta_1 \sin(\theta_1) = -\int_{-1}^{+1} d\cos\theta := \int_{-1}^{1} dx$. Integrating out *all other* n angles θ_i as well as the angle φ gives a $\Omega_{2+n}/2$ contribution, as the $n + 3$-sphere volume is given by $\int d^{3+n}r = \int dr\Omega_{n+2}r^{n+2}$ and we divide by the missing factor $\int_0^\pi d\theta \sin(\theta) = 2$, used for the scalar product substitution. We end up with

$$= \frac{1}{(2\pi)^{3+n}} \frac{\Omega_{n+2}}{2} \int_{-1}^{+1} dx \int_0^\infty dr \; r^{2+n} V(r) \; e^{-irpx} \tag{6.6c}$$

$$= \frac{1}{(2\pi)^{3+n}} \frac{\Omega_{n+2}}{2} \int_0^\infty dr \; r^{2+n} V(r) \left[\frac{1}{-ipr} e^{-iprx} \right]_{-1}^{+1} \tag{6.6d}$$

$$= \frac{1}{(2\pi)^{3+n}} \frac{\Omega_{n+2}}{2} \frac{i}{p} \left(\int_0^\infty dr \; r^{1+n} V(r) e^{-ipr} - \int_0^\infty dr \; r^{1+n} V(r) e^{+ipr} \right) \tag{6.6e}$$

In favour to write this line as an effective one dimensional fourier transform, we transform the second integral in line (6.6e), first by switching the integral borders, $\int_0^\infty dr = -\int_\infty^o dr$, second by variable substitution $r := -r'$. This inserts an alternating minus, depending on n, as $r^{1+n}dr = (-1)^{1+n}(r')^{1+n}(-1)dr' = (-1)^n r'dr'$. Note the substitution also toggles the sign of the integral borders, allowing to combine both integrals to

$$= \frac{1}{(2\pi)^{3+n}} \frac{\Omega_{n+2}}{2} \frac{i}{p} \int_{-\infty}^\infty dr \; r^{1+n} \left[V(r)\Theta(r) + (-1)^n V(-r)\Theta(-r) \right] e^{-ipr} \tag{6.6f}$$

$$= \frac{1}{2\pi} \int_{-\infty}^\infty dr \; v(r) \; e^{-ipr}. \tag{6.6g}$$

We derived an effective one dimensional fourier transformation of the effective function

$$v(r) := \frac{1}{(2\pi)^{2+n}} \frac{\Omega_{2+n}}{2} \frac{i}{p} r^{1+n} \left[V(r)\Theta(r) + (-1)^n V(-r)\Theta(-r) \right]. \tag{6.7}$$

Note that the heaviside step function $\Theta(z)$, which was used to combine the integrals from line (6.6e) to one in (6.6f) is understood on the complex plane as

$$\Theta(z) = \Theta(\operatorname{Re} z). \tag{6.8}$$

The requirement (6.8) must be only exactly fulfilled at the evaluation points of the integral, that is, the poles of $v(r)$. Therefore, $\Theta(z)$ may be weaker defined. See appendix 6.2.2 for more details.

Therefore issues may arise with holomorphy when cauchy theorem shall be applied. This is discussed a bit more in the appendix, while we realized that solving the integral on the complex plane works in three dimensions, so it shall work in any higher number of dimensions. Note that this approach was also successfully applied to a GUP-inspired nonlocal operator in onging work [41].

6.2 Deriving the bilocal smearing operator

We now can solve the $\mathcal{A}^{-2}$ integral (6.5d) by rewriting it to an one-dimensional one. Inserting

$$V(r) = \frac{1}{\Omega_{n+2} r^{n+2}} \frac{\mathrm{d}H(r)}{\mathrm{d}r} \tag{6.9}$$

into equation (6.6f) results in the compact expression, valid for any dimension n:

$$\mathcal{A}^{-2}(p^2) = \frac{1}{(2\pi)^{3+n}} \frac{i}{2p} \int_{-\infty}^{\infty} \mathrm{d}r \frac{H'(|r|)}{r} e^{-ipr}. \tag{6.10}$$

We now plan to solve this equation with residue theorem. Since in (6.10), $r \equiv \|\vec{r}\| \geq 0$ and $p \equiv \|\vec{p}\| \geq 0$, there is only one integration contour for Jordan's lemma. For the forward Fourier transformation $\mathcal{F}_1$, as seen in (6.10), the contour is determined by requiring

$$\lim_{r \to \pm i\infty} e^{-ipr} = 0 \;\Rightarrow\; e^{-i(+\#)(\pm i\infty)} = e^{\pm\infty\#} = 0 \;\Rightarrow\; r \to -i\infty, \tag{6.11}$$

i.e. it is closed on the lower half complex plane ($Im\, r < 0$). For the inverse Fourier transformation $\mathcal{F}_1^{-1}$, it is closed on the upper half complex plane ($p \to i\infty \Leftrightarrow Im\, p > 0$).

6.2.1 Holographic modified Einstein equations

In the holographic model, we insert $h(r)$ to derive from (6.10) the expression (note there is no need for powers of L when switching to dimensionless coordinates)

$$\mathcal{A}^{-2}(q^2) = \underbrace{\frac{2+n}{(2\pi)^{3+n}} \frac{i}{2q}}_{f_0} \int_{-\infty}^{\infty} \mathrm{d}z \left[\underbrace{\frac{z^n}{(1+z^{2+n})^2}}_{f_+} \Theta(z) + \underbrace{\frac{(-1)(-z)^n}{(1+(-z)^{2+n})^2}}_{f_-} \Theta(-z) \right] e^{-iqz}. \tag{6.12}$$

Note that the poles of f_+ are the same as for f_-, just mirrored at the imaginary axis $Re(z) = 0$, in symbols $f_+(z) = -f_-(-z)$. The poles of f_+ are given by

$$\left(1+z^{2+n}\right)^2 = 0 \quad\Leftrightarrow\quad z = (-1)^{\frac{1}{2+n}} = \exp\left\{\frac{i\pi + 2\pi i k}{n+2}\right\} \quad \forall k \in \mathbb{N}_0. \tag{6.13}$$

There are $n+1$ unique poles, each to be counted two times due to the power 2 in the denominator of f_+. Due to the integration contour (6.11), only the $\frac{n+1}{2}$ unique poles in the region $Im(z_0) \leq 0$ are taken into account. For f_+, only the $\frac{n+1}{4}$ poles in the region $Re(z_0) \geq 0$ are visible. We identify these poles by their set of angles in the complex phase,

$$\Phi_n = \left\{ \varphi = \arg(z) \;:\; 1 + z^{n+2} = 0 \wedge Im(z) \leq 0 \wedge Re(z) \geq 0 \right\} \tag{6.14}$$

$$= \left\{ \varphi = \pi \frac{1-2k}{n+2} \;:\; k \in \mathbb{N}_0 \wedge k \leq \frac{n}{4} \right\}, \tag{6.15}$$

and write $e^{i\Phi_n} = \{z = e^{i\varphi} : \varphi \in \Phi_n\}$ to denote the set of complex numbers associated with Φ_n. Note the number of angles $|\Phi_n| = \lfloor \frac{n+1}{4} \rfloor$ is a step-function.

All poles $z_0 \in e^{i\Phi_n}$ are of 2nd order, the residues are therefore given by

$$\operatorname*{Res}_{z \to z_0} f_+(z)e^{iqz} = \lim_{z \to z_0} \frac{\mathrm{d}}{\mathrm{d}z}(z-z_0)^2 f_+(z)e^{iqz} = \frac{\operatorname{sign}(z_0)\bar{z}_0}{(n+2)}e^{iz_0 q}(1-iz_0 q) \tag{6.16}$$

and enter the holographic $\mathcal{A}^{-2}$ integral from (6.12) in a way that

$$\int \mathrm{d}z \, (f_+(z)\Theta(z) + f_-(z)\Theta(-z)) \, e^{iqz} = (2\pi i)(-1)\cdot$$
$$\cdot \left(2 \sum_{z_0 \in e^{i\Phi_n}} \operatorname*{Res}_{z \to z_0} f_+(z) + 2 \sum_{z_0 \in e^{\Phi_n}} \operatorname*{Res}_{z \to z_0} f_-(z) \right). \tag{6.17}$$

Note that due to symmetry of the poles, there are either poles z_0 (produced by f_+) and $-z_0$ (produced by f_-) which residues sum to the expression

$$\operatorname*{Res}_{z_0} f_+ e^{izq} + \operatorname*{Res}_{-z_0} f_- e^{izq} = \operatorname*{Res}_{z_0} f_+ e^{izq} - \operatorname*{Res}_{z_0} f_+ e^{-izq} = \frac{2i\bar{z}_0}{(2+n)^2}\sin(z_0 q), \tag{6.18}$$

or the f_+ and f_- share a common pole at $z_0 = -i$, then

$$\operatorname*{Res}_{-i} f_+ e^{izq} = \frac{i}{n+2}e^{+q}(1-q). \tag{6.19}$$

Note that poles at $z_0 = -i$ only occur at integer $n/4$, that is $n = 0, 4, 8, \ldots$. In favour to give a closed form result, we therefore cannot always apply the simplification rules (6.18) and (6.19). The overall result is therefore given by

$$\mathcal{A}^{-2} = \frac{(2\pi)^{2+n}}{q} \sum_{\varphi \in \Phi_n} \operatorname{sign}(z_0)\bar{z}_0 e^{iz_0 q}(1-iz_0 q) \tag{6.20}$$

with $z_0 = e^{i\varphi}$. Without extra dimensions ($n = 0$) is the only case where a purely real result can be given, for $n > 0$ complex phases always survive in (6.20). For $n = 0$ we get (with $q = pL$):

$$\mathcal{A}^{-2} = \frac{1}{4\pi}\left(\frac{e^{-q}}{q} + e^{-q}\right). \tag{6.21}$$

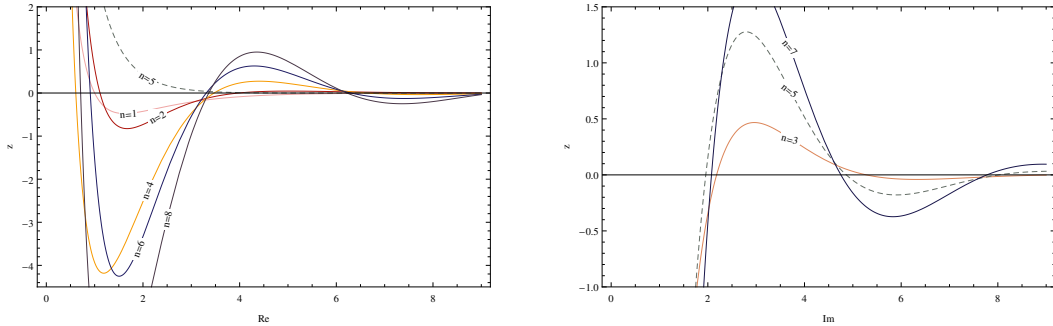Reinserting L and sending $L \to 0$ gives $\mathcal{A}^{-2} \to 1/4\pi$

Figure 6.1: A placeholder picture for the upcoming plot of $\mathcal{A}^{-2}(p)$.

6.2.2 Self-encoding modified Einstein equations

For sef-encoding model, we insert $h_\alpha(r)$ into the integral for $\mathcal{A}^{-2}$ as given in (6.10). For convenience, we switch to a new dimensionless notation, $L' := L/2^{1/\alpha}$ and $z = r/L'$, $q = pL'$. With that notation, all poles will have radius 1. The integral reads:

$$\mathcal{A}^{-2}(q^2) = \underbrace{\frac{3+n}{(2\pi)^{3+n}}\frac{i}{2q}}_{f_0} \int_{-\infty}^{\infty} \mathrm{d}z \left[\underbrace{\frac{z^{1+n}}{(1+z^\alpha)^{\frac{3+n}{\alpha}+1}}}_{f_+} \Theta(z) + \underbrace{\frac{(-1)(-z)^{1+n}}{(1+(-z)^\alpha)^{\frac{3+n}{\alpha}+1}}}_{f_-} \Theta(-z) \right] e^{-iqz}. \quad (6.22)$$

As with the holographic model, I chose $f_+(z) = -f_-(-z)$ and will therefore discuss only f_+. It's poles are given by

$$(1+z^\alpha)^{\frac{3+n}{\alpha}+1} = 0 \quad \Leftrightarrow \quad z = (-1)^{1/\alpha} = \exp\left\{ \frac{i\pi + 2\pi i k}{\alpha} \right\} \quad \forall k \in \mathbb{N}_0. \quad (6.23)$$

For arbitrary choices of $\alpha \in \mathbb{R}_{\geq 0}$, as they were physically discussed in section 4.4.1, the poles multiplicity in (6.23) is not an integral number. For the poles determination, this is not a problem, but for calculating residues it is.

Equation for nth order singularities of a function $g(z)$:

$$\operatorname*{Res}_{z \to a} g(z) = \frac{1}{(n+1)!} \lim_{z \to a} \frac{\partial^{n-1}}{\partial z^{n-1}} \left((z-a)^n g(z) \right) \quad (6.24)$$

Ways to solve that for $n := \frac{3+n}{\alpha}$: Fractional calculus...

7 Conclusion

In this thesis, I presented two self-encoding black hole geometries with their extra dimensional generalization. The discussion was preceded by an introducion about the topics general relativity, exact solutions, higher dimensional gravity scenarios and the quest for quantum gravity, namely by enumerating six quantum gravity theories that predict black holes.

Considering the geometry of the two self-encoding black holes, I introduced the concept of the black hole *remnant* and showed the parallel to the charged Reissner-Nordström black hole. The deSitter core as quantum vacuum source of outward pressure, stemming against the gravitational collapse, was introduced. For the self-encoding non-regular black hole, in this work refered to as the holographic black hole, the curvature singularity is hidden behind a horizon. This incorporates with the minimal length scenario, where distances smaller than the remnant size L_* and bigger than the reduced planck mass M_* can not be probed. Physics in the trans-Planckian regime therefore get's unaccessible and shielded.

Regarding the thermodynamics of the self-encoding black holes, we found the remnants to be *cold* and *stable* in terms of a vanishing temperature and heat capacity. We found logarithmic quantum corrections for the self-encoding holographic black hole in agreement with Loop Quantum Theory and String Theory. The holographic picture leads to area quantization and finally gives rise to an emergent gravity interpretation, explaining the gravitational force as entropic force.

As a last step, the *dual* theory to the self-encoding black holes was constructed, by means of finding the nonlocal operator that, applied on a clueless Diracian, produces just the desired distortion. This is a doorway of bringing the theory on a more fundamental level.

An appealing property of the geometries in this work is that one can do "paper and pen physics" without relying on numerical computations from the beginning. With the distinct feature of extra dimensions, we feel this work pushes the original work forward on the "route to testable predictions" [53].

Minimal length is open to discussion [16].

Experimental: Gravitational tests of GUP [62]; Spalluci BH production? [63]

A   All forms of H

The choice $H(r) = h(r)$ is called *holographic model* and the choice $H(r) = h_\alpha(r)$ is called *self-encoding model* in this thesis. They are distinguished by the index α on the h. Of course, one could also introduce a symbol like $h_n(r)$ to account the fact that the models scale with n, so evventually the symbol is arbitrary.

In this appendix, we give the full forms in the dimensionless notation $z = r/L$. Since the models $H(r)$ represent a smeared Theta function, they are dimensionless, and the identity $h(r) = h(r/L)$ shall represent the fact that $h(r)$ is actually a function of r/L and can be expressed in the dimensionless coordinate $h(z)$:

$$h(r) = \frac{r^{2+n}}{r^{2+n} + L^{2+n}} \qquad\qquad h(z) = \frac{1}{1 + \left(\frac{1}{z}\right)^{2+n}} = \frac{z^{2+n}}{z^{2+n} + 1} \qquad (A.25)$$

$$h_\alpha(r) = \frac{r^{3+n}}{(r^\alpha + L^\alpha/2)^{\frac{3+n}{\alpha}}} \qquad\qquad h_\alpha(z) = \frac{1}{\left(1 + \left(\frac{1}{z}\right)^\alpha /2\right)^{\frac{3+n}{\alpha}}} \qquad (A.26)$$

The derivatives appear in many places and are therefore denoted here. Since $\frac{\mathrm{d}f}{\mathrm{d}r} = \frac{\mathrm{d}f}{\mathrm{d}z}\frac{\mathrm{d}z}{\mathrm{d}r} = \frac{1}{L}\frac{\mathrm{d}f}{\mathrm{d}z}$, we can always substitute $H'(r) = H'(z)/L$. It is important to remember this fact: $H'(r) \neq H'(z)$. In the end, this is because the Lagrange differential operation notation H' is not unique.

$$h'(r) = \frac{(2+n)\, r^{1+n} L^{2+n}}{(r^{2+n} + L^{2+n})^2} \qquad\qquad h'(z) = \frac{(2+n)\left(\frac{1}{z}\right)^{3+n}}{\left(1 + \left(\frac{1}{z}\right)^{2+n}\right)^2} = (2+n)\frac{h^2(z)}{z^{3+n}} \qquad (A.27)$$

$$h'_\alpha(r) = \frac{(3+n)L^\alpha r^{n+2}\left(\frac{L^\alpha}{2} + r^\alpha\right)^{-\frac{n+3}{\alpha}}}{L^\alpha + 2r^\alpha} \qquad h'_\alpha(z) = \frac{\frac{3+n}{2}\left(\frac{1}{z}\right)^{\alpha+1}}{\left(1 + \left(\frac{1}{z}\right)^\alpha /2\right)^{\frac{3+n}{\alpha}+1}} \qquad (A.28)$$

The dimensional analysis allows to resemble the powers of L in any expression written in terms of z. For example, the quantity $H'(z)/z$ has the unit $1/L^2$ and therefore $H'(z)/(zL^2) = H'(r)/r$.

(a) Holographic $h'(r)$ in different LXDs n (b) Self-encoding $h'_\alpha(r)$ in $n = 2$ for different α
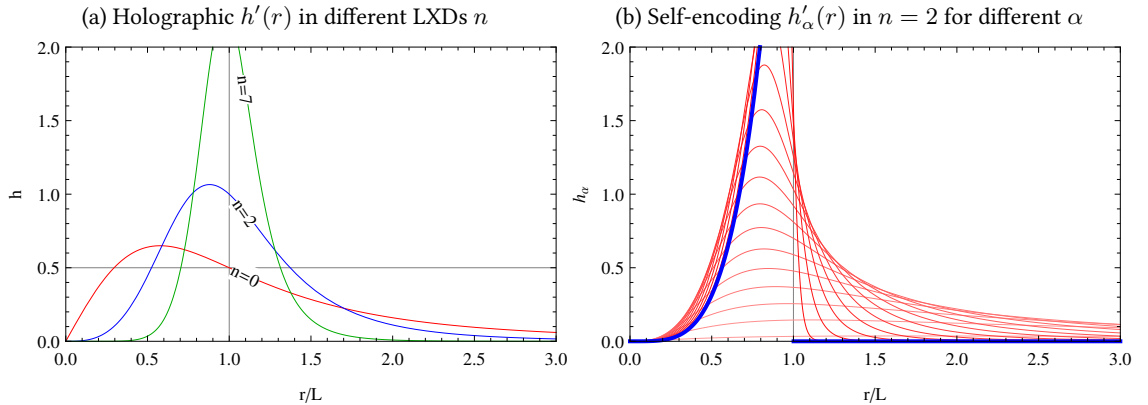
Figure A.2: The delta approximation functions in units of $z = r/L$. One clearly sees that a finite $L > 0$ produces *nonlocality*. These plots just show the derivative of figure 3.3, as $\frac{\mathrm{d}Theta}{\mathrm{d}r} = \delta(r)$.

B n-spheres

To point the emergence of n-spheres in this thesis, we evaluate the d-dimensional volume integral in euclidian space in spherical coordinates $k_i = (r, \phi, \theta_1, \ldots, \theta_{d-2})$, following Wagner [70]:

$$\int \mathrm{d}^d r = \int_0^\infty \mathrm{d}r \, r^{d-1} \underbrace{\int_0^{2\pi} \mathrm{d}\phi \prod_{j=1}^{d-2} \int_0^\pi \mathrm{d}\theta_j \, \sin^j(\theta_j)}_{=a_{n-2}, \text{ since } (n-2)-\text{Surface}} = \frac{2\pi^{d/2}}{\Gamma\left(\frac{d}{2}\right)} \int_0^r \mathrm{d}r \, r^{d-1} := \Omega_{d-1} r^d := V_d \quad \text{(B.29)}$$

where $\Gamma(x)$ is the Euler Gamma function, given by

$$\Gamma(x) = \int_0^\infty \mathrm{d}t \, t^{x-1} e^{-t} \quad \text{; incomplete version:} \quad \gamma(s,x) = \int_0^x t^{s-1} e^t \mathrm{d}t, \quad \Gamma(^1/_2) = \sqrt{\pi}, \quad \text{(B.30)}$$

and the integration of the $d-2$ angles is done with the help of the identities

$$B(x,y) = \int_0^1 \mathrm{d}t \, t^{x-1} (1-t)^{y-1} = \frac{\Gamma(x)\Gamma(y)}{\Gamma(x+y)} \quad \text{(B.31)}$$

$$\int_0^\pi \theta_j \, \sin^j(\theta_j) = \frac{\sqrt{\pi} \, \Gamma\left(\frac{j+1}{2}\right)}{\Gamma\left(\frac{j+2}{2}\right)}. \quad \text{(B.32)}$$

The n-sphere S_n with radius r is defined in an n-dimensional manifold (in this work always the euclidian space) by the set

$$S_n = \{ \, |\mathbf{x}| = r \mid \mathbf{x} \in \mathbb{R} \, \} \quad \text{(B.33)}$$

In this work, the n-sphere is important for integration in spherical coordinates without angular dependence (isotropy or spherical symmetry). Integrating out the angles in a d-dimensional volume integration results in the surface area of the $(d-1)$-sphere, embedded in the d-dimensional space.

Formulas to remember for the volume of an n-Ball and its corresponding $(n-1)$-Sphere:

$$V_n = r^n \frac{\pi^{n/2}}{\Gamma\left(\frac{n}{2}+1\right)} \quad \text{and} \quad A_{(n-1)} = \frac{\mathrm{d}V_n}{\mathrm{d}r} = \frac{\pi^{n/2}}{\Gamma\left(\frac{n}{2}+1\right)} n r^{n-1} = 2 \frac{\pi^{n/2}}{\Gamma\left(\frac{n}{2}\right)} r^{n-1} \quad \text{(B.34)}$$

There also exists recursion relations for determining V_n, A_n by their lower dimensional values. For the sake of completeness, I also give definitions of the Gamma function Γ:

$$\begin{aligned}\Gamma(x) &= (x-1)! \\ \Gamma(x+1) &= x\Gamma(x)\end{aligned} \quad \text{Prefactors:} \quad \begin{aligned}V_n &= v_n r^n \\ A_n &= a_n r^n\end{aligned} \quad \text{Recursion:} \quad \begin{aligned}v_0 &= 1, \quad v_{n+1} = a_n/(n+1) \\ a_0 &= 2, \quad a_{n+1} = 2\pi v_n\end{aligned} \quad \text{(B.35)}$$

I typically split the r-dependence in favour to dimensionless constants by $A_n = \Omega_n r^n$ and $V_n = \mathcal{V}_n r^n$. For numerical values see table B.1.

d	0	1	2	3	4	5	6
$\mathcal{V}_d$	0	2	π	$\frac{4}{3}\pi$	$\frac{1}{2}\pi^2$	$\frac{8}{15}\pi^2$	$\frac{1}{6}\pi^3$
Ω_d	0	2	2π	4π	$2\pi^2$	$\frac{8}{3}\pi^2$	π^3

Table B.1: Volume and surface area prefactors of d-Spheres.

C Details of the radial symmetric d-dimensional FT

This appendix ties up with section 6.1, where the d-dimensional Fourier Transformation is reduced to a one dimensional one for functions $V(\vec{x})$ which fulfill $V(\vec{x}) = V(|\vec{x}|)$.

The 3d case is actually well known in literature and is given here just for completeness and simpler readiness in section 6.2.2. In section 222, we discuss about entire function aspects of $\Theta(z)$.

C.1 Review of the 3d Fourier transformation

We start the derivation in $d = 3$ total spatial dimensions ($\vec{r} \in \mathbb{R}^3$). Let $V = V(r)$ with $r = |\vec{r}|$ be a radially symmetric potential. Then it's fourier transformation is given by:

$$\hat{V}(p) = \frac{1}{(2\pi)^3} \int \mathrm{d}^3 r \; e^{-i\vec{r}\cdot\vec{p}} \, V(r) \tag{C.36a}$$

$$= \frac{1}{(2\pi)^3} \int_0^\infty \mathrm{d}r \int_0^\pi r^2 \sin\theta \, \mathrm{d}\theta \int_0^{2\pi} \mathrm{d}\varphi \; V(r) \, e^{-ipr\cos\theta_2} \tag{C.36b}$$

In line (C.36b) we already wrote the scalar product with an inner angle θ_2. We now substitute the radial angle θ (the θ which is part of $\vec{r} = (r, \theta, \varphi)$) integration with a $\cos\theta$ integration. This can be done because $\frac{\mathrm{d}\cos\theta}{\mathrm{d}\theta} = -\sin\theta$ and so $\int_0^\pi \sin\theta\mathrm{d}\theta = -\int_{-1}^1 \mathrm{d}\cos\theta := \int_{-1}^1 \mathrm{d}x$. We now identify $\cos\theta := x$ with $\cos\theta_1$ because they share the same domain, actually $\theta, \theta_1 \in \{0, \pi\}$ (this is a standard procedure, one can also argue with rotating the coordinate systems). Integrating out $\int_0^{2\pi} \mathrm{d}\varphi = 2\pi$ in mind, we continue with:

$$= \frac{2\pi}{(2\pi)^3} \int_{-1}^{+1} \mathrm{d}x \int_0^\infty \mathrm{d}r \; r^2 \, e^{-irpx} V(r) \tag{C.36c}$$

$$= \frac{1}{(2\pi)^2} \int_0^\infty r^2 \, \mathrm{d}r \, V(r) \left[\frac{1}{-ipr} e^{-iprx} \right]_{-1}^{+1} \tag{C.36d}$$

$$= \frac{1}{(2\pi)^2} \frac{i}{p} \int_0^\infty r \, \mathrm{d}r \, V(r) \left\{ e^{-ipr} - e^{+ipr} \right\} \tag{C.36e}$$

$$= \frac{1}{(2\pi)^2} \frac{i}{p} \left\{ \int_0^\infty r \, \mathrm{d}r \, V(r) e^{-ipr} - \int_0^\infty r \, \mathrm{d}r \, V(r) e^{+ipr} \right\} \tag{C.36f}$$

In line (C.36f), we splitted the integral, and we now make two recastings: At first, switching the integral borders, which inserts one minus: $\int_a^b = -\int_b^a$ in (C.36g). Second, another substitution of the integration parameter $r := -r'$ and therefore $\mathrm{d}r = -\mathrm{d}r'$. The two minus signs kill each other in (C.36h), so $r\mathrm{d}r = r'\mathrm{d}r'$. After substitution, we will call r' again r, which is totally valid.

$$= \frac{1}{(2\pi)^2} \frac{i}{p} \left\{ \int_0^\infty r \, \mathrm{d}r \, V(r) e^{-ipr} + \int_\infty^0 r \, \mathrm{d}r \, V(r) e^{+ipr} \right\} \tag{C.36g}$$

$$= \frac{1}{(2\pi)^2} \frac{i}{p} \left\{ \int_0^\infty r \, \mathrm{d}r \, V(r) e^{-ipr} + \int_{-\infty}^0 r' \, \mathrm{d}r' \, V(-r') e^{-ipr'} \right\} \tag{C.36h}$$

$$= \frac{1}{(2\pi)^2} \frac{i}{p} \int_{-\infty}^\infty r \, \mathrm{d}r \, e^{-ipr} \; \{ V(r)\Theta(r) + V(-r)\Theta(-r) \} \tag{C.36i}$$

$$= \frac{1}{(2\pi)^2} \frac{i}{p} \int_{-\infty}^\infty \mathrm{d}r \; \{ rV(|r|) \} \; e^{-ipr} \tag{C.36j}$$

$$= \frac{1}{2\pi} \int_{-\infty}^\infty \mathrm{d}r \; v(r) \, e^{-ipr} \tag{C.36k}$$

We derived an effective one dimensional fourier transformation of the new function ("kernel")

$$v(r) := \frac{i}{2\pi} \frac{r}{p} V(|r|) \tag{C.37}$$

For shortness, my usual definition of $v(r)$ differs from the one given in (C.37) in terms of non-complex prefactors. For the discussion, equation (C.36i) is the best starting point, as it contains the Heaviside step functions $\Theta(\pm r)$.

The most important issue with this calculation is the question of holomorphy. In these lines, $\Theta(z)$ must be understood as

$$\Theta(z) = \Theta(Re\, z). \tag{C.38}$$

This definition is intrinsically nonholomorphic. On the other hand, as soon as Θ is implemented as a smeared distribution, like continuing the integral of a Dirac delta approximation like the Cauchy distribution, this might be cured. Anyway, there is no ordering relation $\leq_{\mathbb{C}}$ in the complex numbers, so the theta is likely to behave differently on the complex plane. In three dimensions this approach is well known and works.

Whats about the real and complex parts of this fourier transformation? By construction, $V(|r|)$ is an even function (definition: $f(x) = f(-x)$ is even, $-f(x) = f(-x)$ is odd). Therefore $r\, V(|r|)$ is an odd function. By Eulers formula $e^{i\varphi} = \cos\varphi + i\sin\varphi$, one quickly finds that the Fourier Transform of an even function includes only (also even) $\cos$ terms and the complex part vanishes, while the FT of an odd function only contains $\sin$ terms and the real part vanishes. The integral in (C.36j) is therefore ony complex, $\int \mathrm{d}r\; rV(|r|)e^{-ipr} \in \mathbb{C} \setminus \mathbb{R}$. But the prefactor makes the final result in (C.36j) completely real again. This can help as a quick check wether the computed result of the integral is correct.

C.2   Analytic continuation of the Heaviside step function

The step function $\Theta : \mathbb{R} \to \mathbb{R}$, as given in

$$\Theta(x) = \begin{cases} 0 & \text{when} \quad x < 0 \\ 1 & \qquad\qquad x \geq 0 \end{cases}, \tag{3.27 revisited}$$

obviously cannot be simply extended on the complex plane. Anyway, in section 6.1, we already formulated *weaker constraints* instead of $\Theta(z) = \Theta(Re\, z)$, namely

- Step function behaviour only on the poles which are laid on the unit ring $|z| = 1$

- Approximate step function behaviour.

- Freedom of poles for $\Theta(z)$, so it does not contribute with poles to $v(z)$.

Freedom of poles means, we cannot have a rational function, so all theta approximations introduced in this thesis leave the stage. Such a theta approximation may be given by

$$\Theta_k(z) = \frac{1}{1 + \exp(-2kz)}, \quad \text{and}\;\; \Theta(x) = \lim_{k\to\infty} \Theta_k(x) \;\text{ for } x \in \mathbb{R} \tag{C.39}$$

Inserting $z = e^{i\phi}$ gives... okay this is not true.

D   Detailed Tensors in the spherical symmetry calculation and a formulary

In this section, I use greek lowercase letters $(\alpha\beta \ldots \mu\nu \ldots)$ for all indices which may in general be running in 4 or $4+n$ dimensions. Einstein sum convention is used, but summation symbols are given when special emphazise on the summation is intended.

1. Christoffels for Tensor

$$\Gamma^k_{ij} = \frac{g^{kl}}{2}\left(\partial_i g_{jl} + \partial_j g_{il} - \partial_l g_{ij}\right) \tag{D.40}$$

2. Christoffel symmetry:
$$\Gamma^{\alpha}_{\beta\gamma} = \Gamma^{\alpha}_{\gamma\beta} \tag{D.41}$$

3. Covariant derivative for covariant vector t:
$$\nabla_a t^\nu = \partial_a t^\nu + \Gamma^\nu_{ac} t^c \tag{D.42}$$

4. Covariant derivative for a $(2,0)$ tensor A:
$$\nabla_\lambda A^{\mu\nu} = \sum_\delta \partial_\lambda A^{\mu\nu} + \Gamma^\mu_{\delta\lambda} A^{\delta\mu} + \Gamma^\nu_{\delta\lambda} A^{\mu\delta} \tag{D.43}$$

5. Covariant derivative for a $(1,1)$ tensor A:
$$\nabla_a T^b_c = \partial_a T^b_c + \Gamma^b_{ad} T^d_c - \Gamma^d_{ac} T^a_d \tag{D.44}$$

6. Energy conservation equation with sums
$$\sum_\mu \nabla_\mu T^{\mu\nu} = \sum_{\mu,\rho} \partial_\mu T^{\mu\nu} + \Gamma^\mu_{\rho\mu} T^{\rho\mu} + \Gamma^\nu_{\rho\mu} T^{\mu\rho} \tag{D.45}$$

7. Lowering and raising indices
$$g_{\beta\gamma} A^{\alpha\gamma} = A^\alpha_\beta \tag{D.46}$$

8. Metric identity
$$g^{\alpha\beta} g_{\beta\gamma} = g_{\gamma\beta} g^{\beta\alpha} = \delta^\alpha_\gamma \tag{D.47}$$

9. Riemann Tensor
$$R^\delta_{\sigma\mu\nu} = \partial_\mu \Gamma^\delta_{\nu\sigma} - \partial_\nu \Gamma^\delta_{\mu\sigma} + \Gamma^\delta_{\mu\gamma} \Gamma^\gamma_{\nu\sigma} - \Gamma^\delta_{\nu\gamma} \Gamma^\gamma_{\mu\sigma} \tag{D.48}$$

10. Ricci tensor (sign is convention)
$$R_{\mu\nu} = \pm R^\gamma_{\mu\gamma\nu} \tag{D.49}$$

11. $(1,1)$-form of Ricci tensor
$$R^a_b = g^{ca} R_{cb} \tag{D.50}$$

D.1 Christoffel symbols

The Christoffel symbols for a general d-dimensional isotropic static metric, the parametrization $g_{tt} = -(1 - A(r))$, $g_{rr} = 1/(1 - A(r))$ and the alternative parametrization $g_{tt} = -e^{\nu(r)}$, $g_{rr} = g^{-\nu(r)}$. The index naming convention follows section 3. f' indicates the derivation $\partial_r f(r)$.

$$\Gamma^t_{tr} = \Gamma^t_{rt} = \frac{1}{2} g^{tt} \partial_r g_{tt} \quad = \frac{1}{2} \frac{A'}{A-1} \quad\quad = \frac{\nu'}{2} \tag{D.51}$$

$$\Gamma^r_{tt} = \frac{1}{2} g^{rr} \partial_r g_{tt} \quad = \frac{1}{2}(A-1)A' \quad = \frac{1}{2} e^{2\nu} \nu' \tag{D.52}$$

$$\Gamma^r_{rr} = \frac{1}{2} g^{rr} \partial_r g_{rr} \quad = \frac{1}{2} \frac{A'}{1-A} \quad\quad = -\frac{1}{2}\nu' \tag{D.53}$$

$$\Gamma^i_r i = \Gamma^i_{ir} = \frac{1}{2} g^{ii} \partial_r g_{ii} \quad = \frac{1}{r} \tag{D.54}$$

$$\Gamma^i_{\phi\phi} = \frac{1}{2} g^{ii} \partial_i g_{ii} \quad = -\cos(\theta_i)\sin(\theta_i) \tag{D.55}$$

$$\Gamma^\phi_{r\phi} = \Gamma^\phi_{\phi r} = \frac{1}{2} g^{\phi\phi} \partial_r g_{\phi\phi} = \frac{1}{r} \tag{D.56}$$

$$\Gamma^\phi_{\phi i} = \Gamma^\phi_{i\phi} = \frac{1}{2} g^{\phi\phi} \partial_i g_{\phi\phi} = \frac{1}{\tan(\theta_i)} \tag{D.57}$$

8 List of figures and tables

This list helps to find and identify figures; they are labeled by their size and type (illustration or plots) and marked if they were not self-made.

8.1 List of figures

Chapter 9

Bibliography

[1] Ansoldi, Stefano, "Spherical black holes with regular center: A Review of existing models including a recent realization with Gaussian sources", *arXiv*, e-print, (2008). [arXiv:0802.0330 [gr-qc]]. (Cited on pages 26, 28, 30, 31, 32, and 52.)

[2] Ashtekar, Abhay and Lewandowski, Jerzy, "Background independent quantum gravity: A Status report", *Class.Quant.Grav.*, **21**, R53 (2004). [DOI], [arXiv:gr-qc/0404018 [gr-qc]]. (Cited on page 18.)

[3] Aurilia, A. and spallucci, E., "Planck's uncertainty principle and the saturation of Lorentz boosts by Planckian black holes", *arXiv*, e-print, (2013). [arXiv:1309.7186 [gr-qc]]. (Not cited.)

[4] Aurilia, Antonio and Spallucci, Euro, "Why the length of a quantum string cannot be Lorentz contracted", *Adv.High Energy Phys.*, **2013**, 531696 (2013). [DOI], [arXiv:1309.7741 [hep-th]]. (Not cited.)

[5] Barvinsky, A.O., "Nonlocal action for long distance modifications of gravity theory", *Phys.Lett.*, **B572**, 109–116 (2003). [DOI], [arXiv:hep-th/0304229 [hep-th]]. (Cited on page 17.)

[6] Barvinsky, A.O., "Aspects of Nonlocality in Quantum Field Theory, Quantum Gravity and Cosmology", *arXiv*, e-print, (2014). [arXiv:1408.6112 [hep-th]]. (Cited on page 17.)

[7] Bekenstein, Jacob D. and Kamajian, Alfred T., "Information in the Holographic Universe", *Scientific American*, (December 17, 2005), p. ... (Cited on pages 39 and 52.)

[8] Bleicher, Marcus and Nicolini, Piero, "Large Extra Dimensions and Small Black Holes at the LHC", *J.Phys.Conf.Ser.*, **237**, 012008 (2010). [DOI], [arXiv:1001.2211 [hep-ph]]. (Cited on page 14.)

[9] Bleicher, Marcus and Nicolini, Piero, "Mini-review on mini-black holes from the mini-Big Bang", *Astron. Nachr.*, **335**, 605–611 (2014). [DOI], [arXiv:1403.0944 [hep-th]]. (Cited on pages 14 and 15.)

[10] Bonanno, A. and Reuter, M., "Spacetime structure of an evaporating black hole in quantum gravity", *Phys.Rev.*, **D73**, 083005 (2006). [DOI], [arXiv:hep-th/0602159 [hep-th]]. (Cited on page 18.)

[11] Carr, B.J., "The Black Hole Uncertainty Principle Correspondence", *arXiv*, e-print, (2014). [arXiv:1402.1427 [gr-qc]]. (Cited on page 18.)

[12] Carr, Bernard, Modesto, Leonardo and Premont-Schwarz, Isabeau, "Generalized Uncertainty Principle and Self-dual Black Holes", *arXiv*, e-print, (2011). [arXiv:1107.0708 [gr-qc]]. (Cited on page 18.)

[13] Casadio, R., "What is the Schwarzschild radius of a quantum mechanical particle?", *arXiv*, e-print, (2013). [arXiv:1310.5452 [gr-qc]]. (Not cited.)

[14] Casadio, Roberto, Micu, Octavian and Nicolini, Piero, "Minimum length effects in black hole physics", *arXiv*, e-print, (2014). [arXiv:1405.1692 [hep-th]]. (Not cited.)

[15] Cavaglia, Marco, "Black hole and brane production in TeV gravity: A Review", *Int.J.Mod.Phys.*, **A18**, 1843–1882 (2003). [DOI], [arXiv:hep-ph/0210296 [hep-ph]]. (Cited on pages 14, 15, and 52.)

[16] Dirkes, Alain R. P., Maziashvili, Michael and Silagadze, Zurab K., "Black hole remnants due to Planck-length deformed QFT", *arXiv*, e-print, (2013). [arXiv:1309.7427 [gr-qc]]. (Cited on page 46.)

[17] Dvali, Gia and Gomez, Cesar, "Self-Completeness of Einstein Gravity", *arXiv*, e-print, (2010). [arXiv:1005.3497 [hep-th]]. (Not cited.)

[18] Dvali, Gia and Gomez, Cesar, "Self-Completeness of Einstein Gravity", *arXiv*, e-print, (2010). [arXiv:1005.3497 [hep-th]]. (Not cited.)

[19] Dvali, G. and Gomez, C., "Minimal length and black hole area quantization", *Fortsch.Phys.*, **59**, 579–585 (2011). [DOI]. (Cited on page 40.)

[20] Dvali, Gia and Gomez, Cesar, "Black Hole's Quantum N-Portrait", *Fortsch.Phys.*, **61**, 742–767 (2013). [DOI], [arXiv:1112.3359 [hep-th]]. (Cited on page 40.)

[21] Dymnikova, Irina, "Cosmological term as a source of mass", *Class.Quant.Grav.*, **19**, 725–740 (2002). [DOI], [arXiv:gr-qc/0112052 [gr-qc]]. (Cited on pages 26 and 29.)

[22] Elizalde, Emilio and Hildebrandt, Sergi R., "The Family of regular interiors for nonrotating black holes with T0(0)=T1(1)", *Phys.Rev.*, **D65**, 124024 (2002). [DOI], [arXiv:gr-qc/0202102 [gr-qc]]. (Cited on page 29.)

[23] Emparan, Roberto and Reall, Harvey S., "Black Holes in Higher Dimensions", *Living Rev.Rel.*, **11**, 6 (2008). [arXiv:0801.3471 [hep-th]]. (Cited on page 12.)

[24] Falls, Kevin, Litim, Daniel F. and Raghuraman, Aarti, "Black Holes and Asymptotically Safe Gravity", *Int.J.Mod.Phys.*, **A27**, 1250019 (2012). [DOI], [arXiv:1002.0260 [hep-th]]. (Cited on page 18.)

[25] Fließbach, T., *Allgemeine Relativitätstheorie*, Spektrum Lehrbuch, 5. Auflage, (Spektrum-Akademischer Vlg, Heidelberg, 2006). (Cited on pages 7 and 9.)

[26] Frolov, V. and Novikov, I.D., *Black Hole Physics: Basic Concepts and New Developments*, Fundamental Theories of Physics, (Springer Netherlands, 1998). (Cited on page 16.)

[27] Giddings, Steven B., "Possible observational windows for quantum effects from black holes", *arXiv*, e-print, (2014). [arXiv:1406.7001 [hep-th]]. (Not cited.)

[28] Gingrich, Douglas M., "Noncommutative geometry inspired black holes in higher dimensions at the LHC", *JHEP*, **1005**, 022 (2010). [DOI], [arXiv:1003.1798 [hep-ph]]. (Not cited.)

[29] Goenner, Hubert F. M., "On the History of Unified Field Theories", *Living Reviews in Relativity*, **7**(2) (2004). [DOI]. URL (accessed September 2014):
http://www.livingreviews.org/lrr-2004-2. (Cited on page 12.)

[30] Griffiths, J.B. and Podolský, J., *Exact Space-Times in Einstein's General Relativity*, Cambridge Monographs on Mathematical Physics, (Cambridge University Press, Cambridge, 2009). (Cited on pages 10, 11, 12, and 30.)

[31] Hayward, Sean A., "Formation and evaporation of regular black holes", *Phys.Rev.Lett.*, **96**, 031103 (2006). [DOI], [arXiv:gr-qc/0506126 [gr-qc]]. (Cited on pages 28, 31, and 52.)

[32] Isi, Maximiliano, Mureika, Jonas and Nicolini, Piero, "Self-Completeness and the Generalized Uncertainty Principle", *JHEP*, **1311**, 139 (2013). [DOI], [arXiv:1310.8153 [hep-th]]. (Cited on page 18.)

[33] Isi, Maximiliano, Mureika, Jonas and Nicolini, Piero, "Self-Completeness in Alternative Theories of Gravity", *arXiv*, e-print, (2014). [arXiv:1402.3342 [hep-th]]. (Cited on page 18.)

[34] Kanti, Panagiota, "Black holes in theories with large extra dimensions: A Review", *Int.J.Mod.Phys.*, **A19**, 4899–4951 (2004). [DOI], [arXiv:hep-ph/0402168 [hep-ph]]. (Cited on page 14.)

[35] Kanti, Panagiota and Winstanley, Elizabeth, "Hawking Radiation from Higher-Dimensional Black Holes", *arXiv*, e-print, (2014). [arXiv:1402.3952 [hep-th]]. (Cited on pages 13 and 14.)

[36] Kempf, Achim, Mangano, Gianpiero and Mann, Robert B., "Hilbert space representation of the minimal length uncertainty relation", *Phys.Rev.*, **D52**, 1108–1118 (1995). [DOI], [arXiv:hep-th/9412167 [hep-th]]. (Cited on page 18.)

[37] Kiefer, Claus, "Quantum gravity: General introduction and recent developments", *Annalen Phys.*, **15**, 129–148 (2005). [DOI], [arXiv:gr-qc/0508120 [gr-qc]]. (Cited on page 19.)

[38] Kiefer, Claus, *Quantum gravity*, International series of monographs on physics, 136, (Oxford Univ. Press, Oxford [u.a.], 2007), 2. ed. edition. (Cited on page 19.)

[39] Koch, Benjamin, *Black hole production and graviton emission in models with large extra dimensions*, Ph.D. thesis, (Goethe-Universität Frankfurt, Frankfurt, 2007). [ADS]. (Cited on pages 7 and 8.)

[40] Koch, Benjamin, Bleicher, Marcus and Hossenfelder, Sabine, "Black hole remnants at the LHC", *JHEP*, **0510**, 053 (2005). [DOI], [arXiv:hep-ph/0507138 [hep-ph]]. (Cited on pages 14, 15, and 52.)

[41] Köppel, Sven, Iso, Maximiliano, Knipfer, Marco, Mureika, Jonas and Nicolini, Piero, "Self-Completeness and the Generalized Uncertainty Principle in Extra Dimensions", in preparation, (2014). (Cited on pages 18 and 43.)

[42] Maldacena, Juan Martin, "Black holes in string theory", *arXiv*, e-print, (1996). [arXiv:hep-th/9607235 [hep-th]]. (Cited on page 19.)

[43] Misner, Charles, Thorne, Kip and Wheeler, John, *Gravitation*, (W. H. Freeman, New York, 1973). (Cited on pages 9, 11, and 30.)

[44] Modesto, Leonardo, "Loop quantum black hole", *Class.Quant.Grav.*, **23**, 5587–5602 (2006). [DOI], [arXiv:gr-qc/0509078 [gr-qc]]. (Cited on page 18.)

[45] Modesto, Leonardo, "Super-renormalizable Quantum Gravity", *Phys.Rev.*, **D86**, 044005 (2012). [DOI], [arXiv:1107.2403 [hep-th]]. (Cited on page 17.)

[46] Modesto, Leonardo, Moffat, John W. and Nicolini, Piero, "Black holes in an ultraviolet complete quantum gravity", *Phys.Lett.*, **B695**, 397–400 (2011). [DOI], [arXiv:1010.0680 [gr-qc]]. (Cited on pages 16 and 31.)

[47] Myers, Robert C., "Tall tales from de Sitter space", in Gomberoff, A. and Marolf, D., eds., *Lectures on Quantum Gravity*, Series of the Centro De Estudios Científicos, p. 12345. Springer, (2006). (Cited on page 12.)

[48] Nicolini, Piero, "Noncommutative Black Holes, The Final Appeal To Quantum Gravity: A Review", *Int.J.Mod.Phys.*, **A24**, 1229–1308 (2009). [DOI], [arXiv:0807.1939 [hep-th]]. (Cited on page 17.)

[49] Nicolini, Piero, "Entropic force, noncommutative gravity and un-gravity", *Phys.Rev.*, **D82**, 044030 (2010). [DOI], [arXiv:1005.2996 [gr-qc]]. (Not cited.)

[50] Nicolini, Piero, "Nonlocal and generalized uncertainty principle black holes", *arXiv*, e-print, (2012). [arXiv:1202.2102 [hep-th]]. (Not cited.)

[51] Nicolini, Piero, Mureika, Jonas, Spallucci, Euro, Winstanley, Elizabeth and Bleicher, Marcus, "Production and evaporation of Planck scale black holes at the LHC", *arXiv*, e-print, (2013). [arXiv:1302.2640 [hep-th]]. (Cited on page 14.)

[52] Nicolini, Piero, Smailagic, Anais and Spallucci, Euro, "Noncommutative geometry inspired Schwarzschild black hole", *Phys.Lett.*, **B632**, 547–551 (2006). [DOI], [arXiv:gr-qc/0510112 [gr-qc]]. (Cited on pages 17 and 20.)

[53] Nicolini, Piero and Spallucci, Euro, "Holographic screens in ultraviolet self-complete quantum gravity", *Adv.High Energy Phys.*, **2014**, 805684 (2014). [DOI], [arXiv:1210.0015 [hep-th]]. (Cited on pages 20, 22, 23, 26, 27, and 46.)

[54] Nicolini, Piero and Spallucci, Euro, "Holographic screens in ultraviolet self-complete quantum gravity", *Adv.High Energy Phys.*, **2014**, 805684 (2014). [DOI], [arXiv:1210.0015 [hep-th]]. (Cited on page 24.)

[55] Nicolini, Piero and Winstanley, Elizabeth, "Hawking emission from quantum gravity black holes", *JHEP*, **1111**, 075 (2011). [DOI], [arXiv:1108.4419 [hep-ph]]. (Cited on page 16.)

[56] Niedermaier, Max and Reuter, Martin, "The Asymptotic Safety Scenario in Quantum Gravity", *Living Reviews in Relativity*, **9**(5) (2006). [DOI]. URL (accessed September 2014):
http://www.livingreviews.org/lrr-2006-5. (Cited on page 18.)

[57] Penrose, Roger, *The large, the small and the human mind*, (Cambridge Univ. Press, Cambridge, 1997). (Cited on pages 5 and 52.)

[58] Perez, Alejandro, "The Spin-Foam Approach to Quantum Gravity", *Living Reviews in Relativity*, **16**(3) (2013). [DOI]. URL (accessed September 2014):
http://www.livingreviews.org/lrr-2013-3. (Cited on page 18.)

[59] Reuter, M., "Nonperturbative evolution equation for quantum gravity", *Phys.Rev.*, **D57**, 971–985 (1998). [DOI], [arXiv:hep-th/9605030 [hep-th]]. (Cited on page 18.)

[60] Rizzo, Thomas G., "Noncommutative Inspired Black Holes in Extra Dimensions", *JHEP*, **0609**, 021 (2006). [DOI], [arXiv:hep-ph/0606051 [hep-ph]]. (Cited on pages 17 and 20.)

[61] Rovelli, Carlo, "Loop Quantum Gravity", *Living Reviews in Relativity*, **11**(5), 12345 (2008). [DOI]. URL (accessed September 2014):
http://www.livingreviews.org/lrr-2008-5. (Cited on page 18.)

[62] Scardigli, Fabio and Casadio, Roberto, "Gravitational tests of the Generalized Uncertainty Principle", *arXiv*, e-print, (2014). [arXiv:1407.0113 [hep-th]]. (Cited on page 46.)

[63] Spallucci, Euro and Smailagic, Anais, "Black holes production in self-complete quantum gravity", *Phys.Lett.*, **B709**, 266–269 (2012). [DOI], [arXiv:1202.1686 [hep-th]]. (Cited on page 46.)

[64] Stephani, Hans, Kramer, Dietrich, Maccallum, Malcolm, Hoenselaers, Cornelius and Herlt, Eduard, *Exact Solutions of Einstein's Field Equations*, Cambridge Monographs on Mathematical Physics, (Cambridge University Press, Cambridge, 2003). (Cited on page 10.)

[65] Susskind, Leonard, "Trouble for remnants", *arXiv*, e-print, (1995). [arXiv:hep-th/9501106 [hep-th]]. (Not cited.)

[66] Susskind, Leonard, "Singularities, Firewalls, and Complementarity", *arXiv*, e-print, (2012). [arXiv:1208.3445 [hep-th]]. (Not cited.)

[67] Susskind, Leonard and Uglum, John, "Black hole entropy in canonical quantum gravity and superstring theory", *Phys.Rev.*, **D50**, 2700–2711 (1994). [DOI], [arXiv:hep-th/9401070 [hep-th]]. (Not cited.)

[68] Thiemann, Thomas, "Lectures on loop quantum gravity", *Lect.Notes Phys.*, **631**, 41–135 (2003). [DOI], [arXiv:gr-qc/0210094 [gr-qc]]. (Cited on page 18.)

[69] Thiemann, Thomas, "Loop Quantum Gravity: An Inside View", *Lect.Notes Phys.*, **721**, 185–263 (2007). [DOI], [arXiv:hep-th/0608210 [hep-th]]. (Cited on page 18.)

[70] Wagner, Marc, "Quantum Field Theory II", lecture notes, (2013). (Cited on pages 18 and 48.)

[71] Wald, Robert M., *General Relativity*, (The University of Chicago Press, Chicago and London, 1984). (Cited on pages 7, 8, 9, 11, and 30.)

[72] Wald, Robert M., "Teaching general relativity", *arXiv*, e-print, (2005). [arXiv:gr-qc/0511073 [gr-qc]]. (Cited on page 7.)

[73] Witten, Edward, "Anti-de Sitter space, thermal phase transition, and confinement in gauge theories", *Adv.Theor.Math.Phys.*, **2**, 505–532 (1998). [arXiv:hep-th/9803131 [hep-th]]. (Cited on page 12.)

10   Erklärung

Ich versichere hiermit, die vorliegende Arbeit selbständig verfasst und keine anderen als die angegebenen Quellen und Hilfsmittel vewendet zu haben. Alle Stellen der Arbeit, die wörtlich oder sinngemäß aus Veröffentlichungen oder aus anderen fremden Texten entnommen wurden, sind von mir als solche kenntlich gemacht worden. Ferner erkläre ich, dass die Arbeit nicht – auch nicht auszugsweise – für eine andere Prüfung verwendet wurde.

Frankfurt am Main, im Oktober 2014

Sven Köppel